Envoy 600 Final Design Report

By

Hermes Aeronautics

Team members: Sung Hyeok Cho, Jordan Chu, Oscar Cruz Carranza, Jesus Cuellar, Sania Esa, Chris Gonzalez, Daniel Molina, Raul Perez, Ervin Rosales

ARO4911L/4912L Aircraft Design

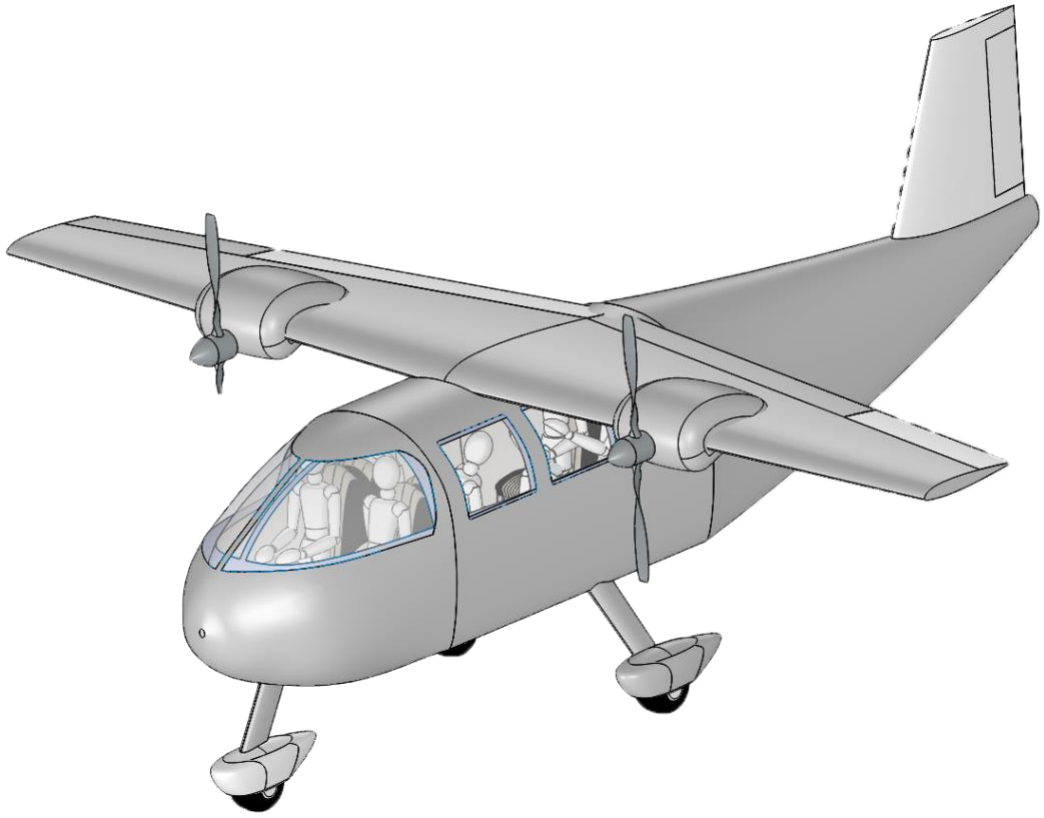

May 12, 2019

Group Member Contributions

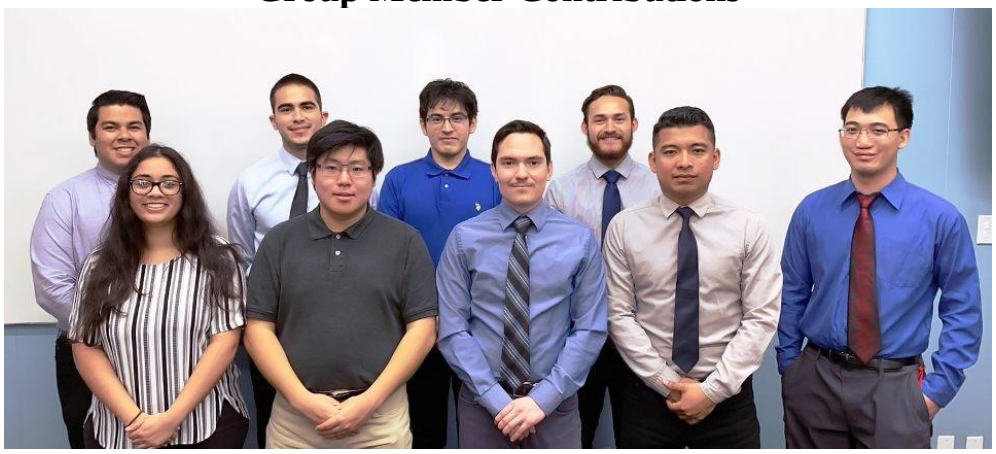

Name	Signature	Responsibility	AIAA NUMBER
Sung Hyeok Cho		Stability and Control Analysis, Propulsion	855669
Jordan Chu		Structure and Loads	762539
Oscar Cruz Carranza		Performance and Stability and Control	985165
Jesus Cuellar		Weights & Balance	985279
Chris Gonzalez		Team Lead, Cost Analysis	985285
Sania Esa		Performance	985146
Daniel Molina		CAD Analyst	867966
Raul Perez		Aerodynamics	985145
Ervin Rosales		Team Deputy, Performance	985159
GRANT CARICHNER		Faculty Advisor	

TABLE OF CONTENTS

LIST OF TABLES

LIST OF FIGURES

LIST OF SYMBOLS

AC − Aerodynamic center
AR − Wing aspect ratio
A_c − Cross-sectional area
α − Angle of attack
b − Span
b_{HT} − Span for horizontal stabilizer
b_{VT} − Span for vertical tail
CG − Center of gravity
C_{HT} − Horizontal tail volume coefficient
$c_{r_{HT}}$ − Root chord for horizontal stabilizer
C_{VT} − Vertical tail volume coefficient
$c_{t_{HT}}$ − Tip chord for horizontal stabilizer
c_r − Root chord
c_t − Tip chord
C_{m_α} − Coefficient of pitching moment caused by angle of attack
C_{l_p} − Coefficient of lateral moment caused by roll rate
C_{n_β} − Coefficient of
$\frac{c_R}{c}$ − Rudder chord to chord ratio
C_d − Section Drag Coefficient
C_l − Section Lift Coefficient
C_L − Lift coefficient
C_D − Drag coefficient
C_{Do} − Zero-lift drag coefficient
δ − Flap deflection
D − Drag
e − Oswald efficiency factor
η_{prop} − Propeller efficiency
H − Height of fuselage
K' − Inviscid drag due to lift factor
K'' − Viscous drag due to lift factor
M_y − Bending moment caused by CG location of fuselage
MAC − Mean Aerodynamic Chord
MAC_{HT} − Mean aerodynamic chord for horizontal stabilizer
MAC_{VT} − Mean aerodynamic chord for vertical stabilizer
MLG −Main landing gear
$MTOW$ − Maximum take-off weight
NLG −Nose landing gear
$N.P.$ −Neutral point
L − Lift
$\frac{P}{W}$ − Power loading
RFP − Request for proposal
σ_b − Ultimate compressive allowable

S – Planform area
S_{WET} – Wetted area
S_g – Ground roll distance
S_R – Rotational distance
S_{TR} – Transition distance
S_{HT} – Horizontal tail area
S_{VT} – Vertical tail area
V_{TO} – Take-off velocity
V_{stall} – Stall speed
θ_{cl} – Climb angle
S_A – Air distance
S_{FR} – Free-roll distance
S_B – Braking distance
V_{TD} – Touchdown velocity
V_{OBS} – Obstacle velocity
V_{EF} – Engine fail velocity
V_R – Rotation speed
V_1 – Decision speed
θ_{app} – Approach angle
Λ_{HT} – Leading edge sweep for horizontal tail
Λ_{LE} – Leading edge sweep
Λ_{TE} – Trailing edge sweep
Λ_{VT} – Leading edge sweep for vertical tail
$\frac{W}{S}$ – Wing loading
x_{CG} – Longitudinal center of gravity location
z_{CG} – Vertical center of gravity location

EXECUTIVE SUMMARY

In today's high paced life, people want to get to where they want as quickly and direct as possible. The aircraft industry has tried to keep up with the demand and also to keep it affordable while also trying to turn a profit. Airlines, over the years, have learned which routes have the highest demand and continually service these areas. This, however, has left dozens if not hundreds of potential routes with less service. With people trying to be efficient as possible, demand has been shown to increase on more frequent routes even if it comes at a higher price tag. AIAA has recognized the need for an aircraft that can service the hundreds of airports currently in the United States and issued the 2018-2019 Undergraduate Thin Haul Transport and Air Taxi RFP. In response to the RFP, Hermes Aeronautics presents the Envoy 600, a high frequency, low acquisition, and low operating cost option for today's aircraft operators.

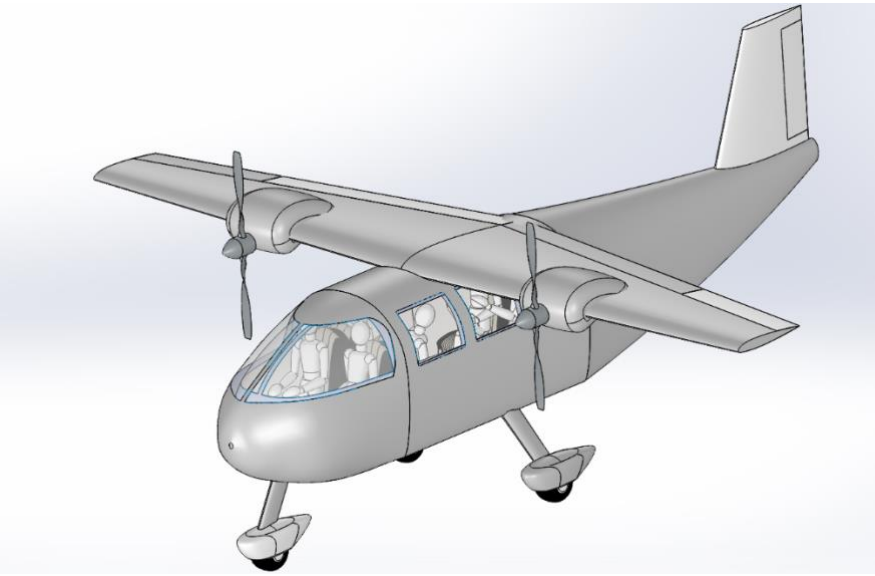

Envoy 600

The Envoy 600 is a 6-seat, high wing aircraft, powered by two Lycoming IO-360-A1A piston engines rated at 200 horsepower each. The overall length is 26.1 feet, has a wing span of 26.8 feet, and has maximum takeoff weight of 3434 pounds. The Envoy 600 meets all the

requirement put forth by the AIAA. It is designed to cruise at an altitude of 8000 feet with a speed of 206 knots which allows the Envoy 600 to achieve the reference mission of 135 nautical miles in 45 minutes, outlined by the RFP. The Envoy 600 is also designed to achieve a larger, sizing mission of 250 nautical miles at full payload capacity in 78 minutes. Takeoff distance and landing distances over a 50-foot obstacle are achieved in 1804 feet and 1411 feet, respectively, which are well below the 2500 foot distances required for both. The Envoy is capable of a 45 minute loiter in the event of a failure to land at 3000 feet.

The Envoy 600 acquisition cost and more importantly, in terms of this RFP, direct operating cost are very competitive when comparing to other aircraft. Based on our current projected production numbers, the Envoy 600 can be acquired between $396,000 and $696,000. We also project the yearly direct operating costs to be $384,000 and $512,000 per year depending on the frequency of use.

With the Envoy 600 being made specifically as a short-range, high frequency aircraft, it has the capability of opening a new, untapped market that is expected to increase in demand as new and establish companies decide to enter. This ultimately gives, consumers more options for direct, low cost flights to that were previously not practical or possible.

1 CONCEPT OF OPERATIONS

1.1 Goal

Hermes Aeronautics' goal is to increase our brand credibility in the aerospace industry by designing, developing, and manufacturing a "Thin-Haul Taxi" plane. This will allow us to break into the on-demand flight market as we develop a platform with low operating costs that will make thin-haul flights economically feasible and attract more customers. In addition, our company wants to generate greater exposure to get bigger contracts in the future.

1.2 Requirements and Constraints

The RFP gave a list of requirements along with requirements for optional deviations to the design. The table below indicates the requirements for the thin haul transport.

Table 1-1 RFP Requirements

Description	**Requirement**
Passenger Capacity	4 passengers with optional deviation of 2-6 passengers
Payload Weight	175 lbs + 25 lbs baggage per passenger. Optional deviation of 2-3 passengers, 180lbs +30 lbs baggage per passenger.
Reference Mission Minimum Average Ground Speed	180 kts
Reference Mission Range (1/2 payload)	Min. 135 nmi
Reference Mission Time for Segments 3-5	Max. 45 min
Sizing Mission Range (Full Payload) for Segments 3-5	Min. 250 nmi
Loiter altitude	3000 ft
Loiter Speed	Best endurance speed
Takeoff and Landing Over Obstacle	50 ft
Takeoff & Landing Length	Max 2500 ft for both takeoff & landing

Technology Readiness	Technologies must be available by 2025
Regulation	Meets certification rules in FAA 14 CFR Part 23
Crew Capacity	Aircraft must contain 1 pilot
Engine Noise limits	Aircraft must meet single engine noise limits even if multi-engine (Part 36 Sec. G36.301(c)
Direct Operating Costs	Lower than current Industry
Battery specific energy (Optional Deviation)	No greater than 285 W-hr/kg - Px85 s
Battery overhaul cost (Optional Deviation)	Minimum $250 per kW-hr every 1000 cycles
Cost of electricity (Optional Deviation)	Minimum $0.10 /kW-hr

1.3 Mission Profile

The mission assigned by the RFP includes takeoff, climb, cruise, descent and land with reserves for an additional climb, loiter, descent, and land. With the additional reserves, the aircraft has the ability to divert safely if it is not safe for the aircraft to land. The mission profile can be seen in figure 1.3-1. The main segments of the mission referred to in the RFP as segments 3-5 are equivalent to segments 2-5 in figure 1.3-1. The RFP's segments 3-5 have time, distance, speed and/or payload restrictions depending on whether it is a sizing or reference mission.

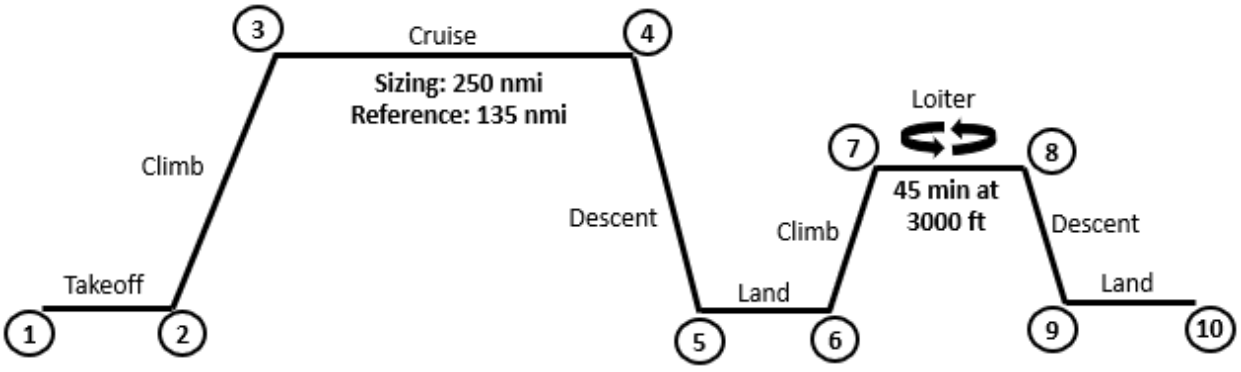

Figure 1.3-1 Initial Sizing Parameters

2 SIZING ANALYSIS

2.1 Initial Sizing

In order to select a design point and calculate initial weight estimates, initial parameters were chosen. Some parameters were given by the RFP whereas others were taken from similar aircrafts or from Ref. [5]. The chosen parameters and their source can be seen in Table 2.1-1 below. For cruise velocity, the RFP stated that the average ground speed for segments 3-5 needed to be either equal to or greater than 180 knots. An initial assumption of 210 knots was chosen based off similar aircraft data.

Table 2-1 Initial Sizing Parameters

Parameter	Value	Unit	Source
Cruise Altitude	3000	Feet	Estimated as minimum for general aviation aircraft
Cruise Distance	250	Nautical Miles	RFP
Cruise Velocity	210	knots	Initial Estimate
Loiter Time	45	Min.	RFP
Pilot	1	-	RFP
Passengers	5	-	RFP
C_{D_o}	0.023	-	From Similar Aircraft
Aspect Ratio	7.5	-	From Similar Aircraft
$C_{L_{max}}$	1.6	-	From Similar aircraft
L/D_{max}	14.75	-	From Similar Aircraft
Takeoff/Landing Field Length	2500	Feet	RFP
c_{BHP} Loiter	0.5		Nicholai and Carichner [5]
c_{BHP} Cruise	0.41		Nicholai and Carichner [5]

2.2 Constraint Analysis

Based on the initial sizing parameters from table 2.1-1, a constraint diagram was made and can be seen in figure 2.2-1 below. The design point was selected with the parameters of 0.11 bhp/lb_f for power loading and 31 lb_f/ft^2 for wing loading and is denoted by the red diamond on the diagram.

This design point was chosen because this point lies in the design space at the lowest power loading.

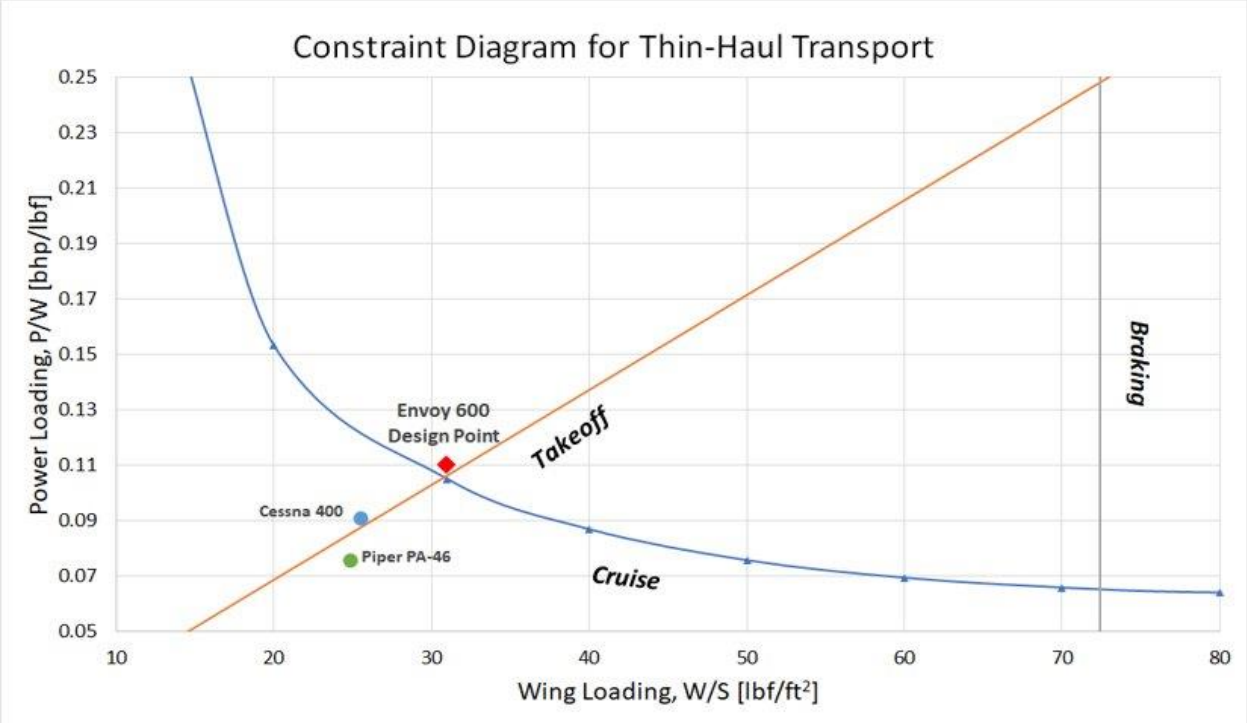

Figure 2.2-1 Constraint Diagram for Thin- Haul Transport

2.3 Initial Weight Estimations

In order to determine an initial max takeoff weight (MTOW) estimate, the following equations including the Breguet Range equations were used to estimate the weight fractions [Ref. 5]. Based off the initial estimations, the aircraft weights were estimated and are presented in Table 2.3-1.

Table 2-2 Initial Weight Estimations

Segments	Weight (lb)
Takeoff Gross Weight	3985
Empty Weight	2072
Zero-Fuel Weight	3252
Full Fuel, No Payload Weight	2985
Fuel Weight	733

These weight estimations were used during the initial stages of design. As the design was refined, weight estimations were checked in a mission analysis program created in excel. The estimations in the above table, using the Breguet Range equations, were higher weight estimations than what was being expected in the mission analysis program. Because of this, further analysis was conducted to select an aspect ratio and aircraft takeoff weight. This study can be seen in section 5.2.1. The new aircraft weight estimations are summarized in Table 2.3-2.

Table 2-3 Refined Initial Weight Estimations

Segments	Weight (lb)
Takeoff Gross Weight	3434
Empty Weight	2197
Zero-Fuel Weight	3197
Full Fuel, No Payload Weight	2434
Fuel Weight	237

3 CONFIGURATION

3.1 Design Morphology

Wing Configuration: Low wing, mid-wing and high wing were considered for wing types. For the Envoy 600, a high wing placement was chosen because it has inherent roll stability, downward visibility, allows good passenger comfort, and ease of passenger loading. A second configuration, the Envoy 600E, was considered for our design. Electric propulsion was considered for this configuration. Due to the higher weight required for an electric propulsion, it was decided this configuration would have low wing placement which requires less structural weight to offset the higher weight of the batteries which would be placed in the wings.

Tail Configuration: Conventional tail, T-tail, V-tail and cruciform tail were considered for the tail type. Conventional tail was chosen as it provides the necessary stability for the mission and has less structural weight.

Landing Gear Type: Tricycle and traditional (tail-wheel) gear were considered for types of landing gear. Tricycle gear was chosen as it provides the necessary stability and weight characteristics. It is easier for ground steering which would make passengers feel more comfortable during landing and takeoff.

Propulsion Type: Based on the velocity and time requirement imposed by the RFP, we choose to go with a piston engine as it is the most efficient engine for this velocity and range. We also considered electric propulsion as an alternative for a second configuration given the relatively short range requirements from the RFP.

3.2 Design Candidate Down-selection

The RFP requires two configurations to be considered and then be down selected to one. The two configurations considered were "Twin Engine Internal Combustion" and "Twin Electric Motor." The two configurations are shown in Figure 3.2-1 and 3.2-2.

Figure 3.2-1 Twin Engine Internal Combustion Configuration

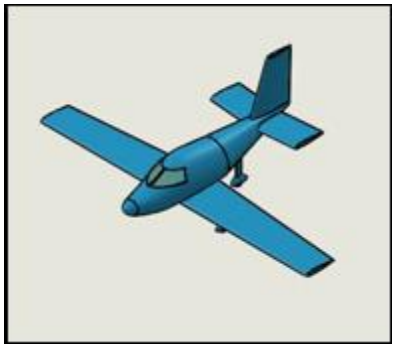

Figure 3.2-2 Twin Electric Motor Configuration

The aircraft down-selection was performed through a trade study, which is shown in Table 3.2-1. Supporting analysis are shown throughout the proposal.

Table 3-1 Configuration Down-selection Trade Study

Weighting Factor	Figure of Merit	Twin Internal Combustion	Twin Electric Motor
0.3	Aircraft Maximum Gross Takeoff Weight	**2** 3434 lb	**1** 12405 lb
0.5	Annual Operating Cost	**2** $186,663	**1** $376,442
0.2	Purchase Cost	**2** $352,000	**1** $701,000
1.0	TOTAL	2.0	1.0

The trade study conclusively showed that the twin internal combustion configuration was a superior choice for the mission. Thus, the twin internal combustion configuration was chosen as the design to be expanded upon while the electric motor configuration was abandoned.

3.3 External Layout

3.3.1 General Sizing

The basic layout of our selected aircraft feature a high wing configuration with a conventional empennage.

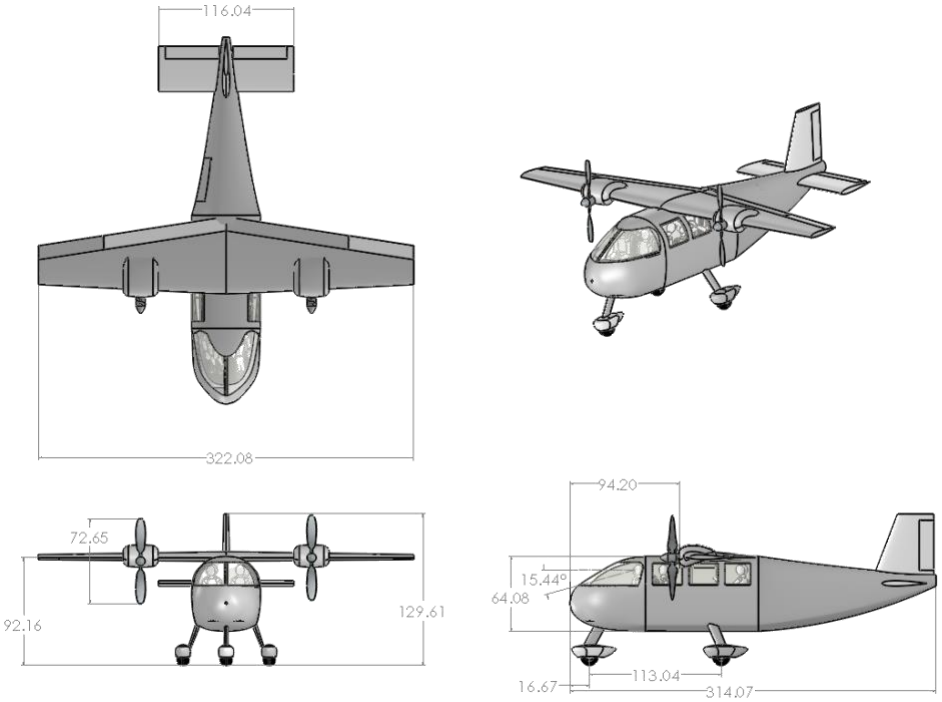

Figure 3.3-1 Three-View Configuration

3.3.2 Engines

Location of the engines was selected to keep them as close to the fuselage centerline as possible to reduce structural weight. Consideration was also given to allow enough clearance for the propellers to rotate freely with ample distance from fuselage. The reduced distance from the centerline of the aircraft proved beneficial in One Engine Inoperable condition as the yawing moment generated by uneven thrust was reduced.

3.3.3 Landing Gear

The landing gear was positioned to prevent aircraft turn over and unwelcome tip back. The height of the struts was determined based on allowing the passengers a comfortable ingress and egress. The landing gear was positioned so that the main landing gear will carry 80-85% of the weight of the aircraft while the nose gear carried the remaining 15-20%. The landing gear will be further discussed later in this report.

3.3.4 Wing & Empennage

A trapezoidal planform was chosen to be the main shape of the wing. The sweep angle of the quarter chord was chosen to be zero as the compressibility effect in the aircraft flight envelope is negligible. The wing was tapered to reduce tip stall which results in a trapezoidal planform. A conventional tail configuration was chosen to reduce any excess structural weight that would have resulted from a nonconventional configuration as the conventional tail configuration was deemed adequate for the mission.

3.3.5 Windows

Visibility for the pilot is important in a design of a manned aircraft. Thus, the cockpit window was designed to provide 15 degrees of vertical field of view below the pilot's horizontal sightline as suggested by Ref [10]. This is illustrated in Figure 3.3.5-1. Six large windows are present in the cabin for passenger visibility, bringing the total window surface area to approximately 2700 in^2.

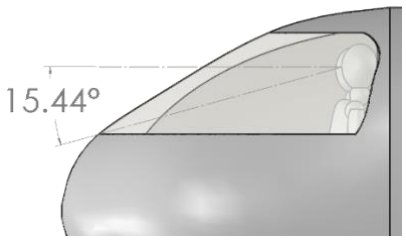

Figure 3.3-2 Viewing Angle

3.3.6 Doors

The main cabin door was sized to allow a sufficient room for a wide variety of passengers. The door was also designed to allow open towards the left without any obstructions guarding its path. Dimensions for the door can be seen in Figure 3.3-3.

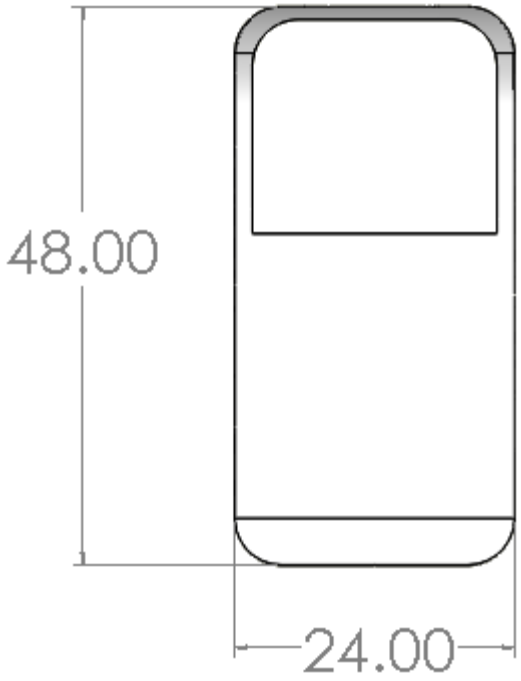

Figure 3.3-3 The main cabin door

3.4 Internal Layout

3.4.1 Fuel Tanks

Similar to the engines, the fuel tanks were stationed near the fuselage centerline to minimize their rolling moment about the fuselage. They have been sized to hold 7.03 ft^3 of aviation gas, which was determined to be sufficient for the larger sizing mission. The position of the fuel tank can be seen in Figure 3.4.4-1.

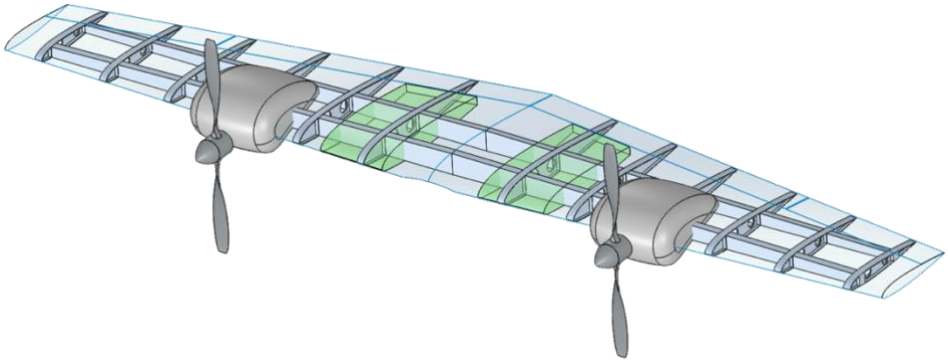

Figure 3.4-1 Positioning of Fuel Tanks

3.4.2 Cabin System

As shown in Figure 3.4.2-1, the cabin will feature three rows by two columns, and is capable of seating 6 occupants, including the pilot. The rearmost rows have been positioned to face each other for an open and friendlier atmosphere.

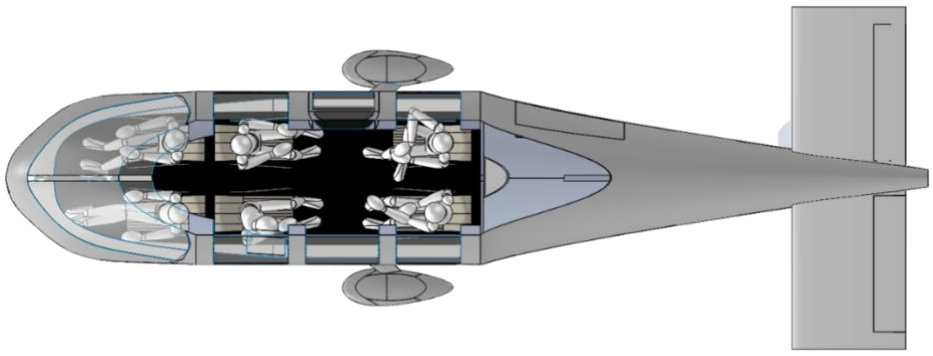

Figure 3.4.2-1 Layout of the Cabin System

3.4.3 Seats

Dimensions for cabin seats were taken from Ref. [10]. They were design to provide a comfortable experience for passengers of every size. Dimensions provided are in inches.

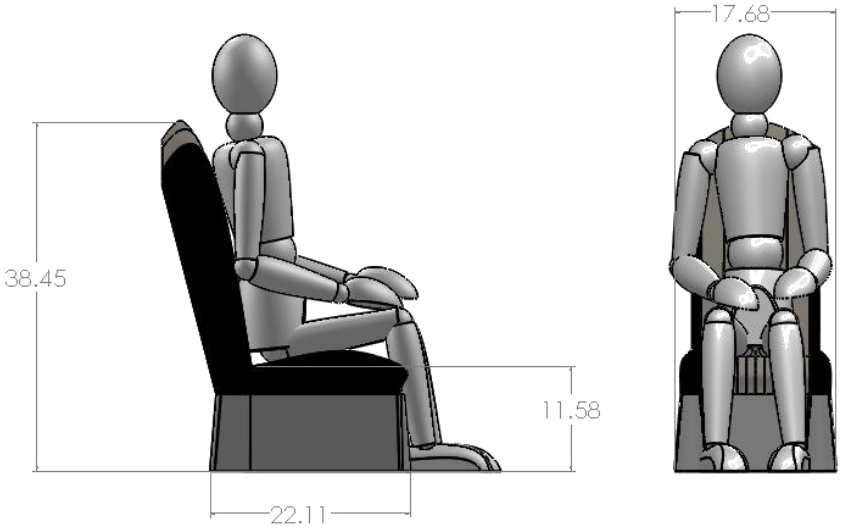

Figure 3.4.4-3.4-2 Illustration of Passengers inside the Cabin

3.4.4 Storage

The storage compartment has been located just aft of the cabin and has been sized to fit 5 travel bags with the dimensions given in Figure 3.4.4-1. The storage compartment can be accessed through a hatch on the starboard side as shown in Figure 3.4.4-2.

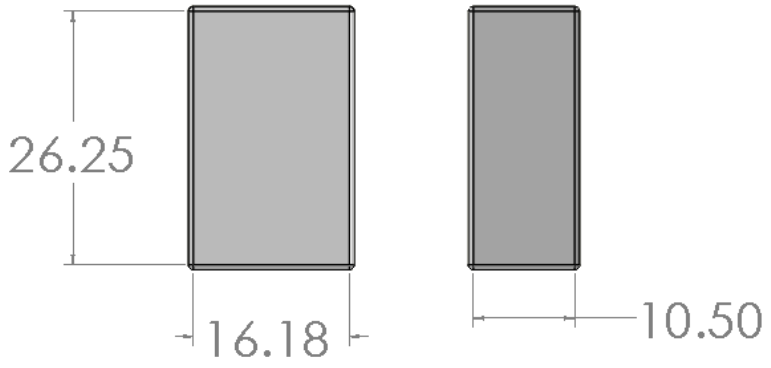

Figure 3.4-3 Dimensions for Luggage

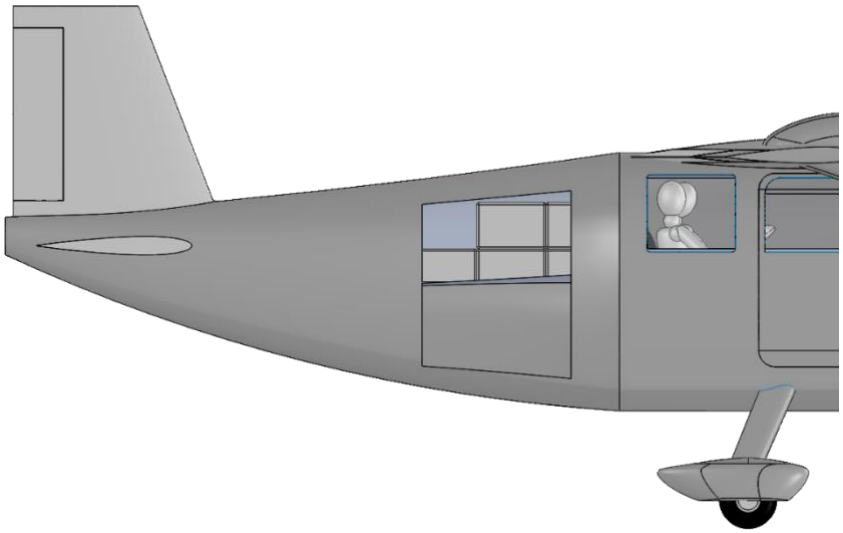

Figure 3.4-4 Access to Storage Compartment

4 PERFORMANCE

4.1 Flight Conditions for Segments 3-5

The RFP requires two missions whose requirements differ based on segments 3-5's time, average ground speed and distance. In addition, the payload for the reference mission was at half payload of 3 passengers and 1 crew and the payload for the sizing mission at full payload of 5 passengers and 1 crew. The cruise altitude and speed selection are discussed in section 4.6. Table 4.1-1 indicates the conditions for segments 3-5.

Table 4-1 Conditions for Segments 3-5

Segment	Reference Speed (kts)	Reference Mission Time (min)	Reference Distance (nmi)	Sizing Speed (kts)	Sizing Mission Time (min)	Sizing Distance (nmi)
Climb	100	4.8	8.75	100	4.8	8.75
Cruise	206	30	103.1	206	63.5	218.1
Descent	139	10	23.1	139	10	23.1
Total	-	44.9	135	-	78.4	250

4.2 Drag per Mission Segment

The drag for each mission segment was calculated and can be seen in table 4.2-1 below. The cruise drag was estimated at our chosen cruise altitude of 8000 feet and the loiter drag at the RFP given altitude of 3000 feet. Takeoff and landing were assumed at sea-level as stated by the RFP. The climb drag was based off an averaged climb velocity.

Table 4-2 Drag per Mission Segment

Segment	Drag (lb)
Takeoff	400
Climb 1 (average)	311
Cruise (at 8000 ft)	428
Climb 2 (average)	302
Loiter (at 3000 ft)	321
Land	390

4.3 Takeoff & Landing Performance

The analysis for takeoff performance was conducted in two distinct ways. The first method, as shown in Figure 4.3-1, utilized the three takeoff segments: ground roll distance (S_G), rotational distance (S_R), and transition distance (S_{TR}). The ground roll segment represents the distance covered in the time it takes the aircraft to reach takeoff velocity, V_{TO}. Takeoff velocity was determined to be 1.2 times the calculated takeoff stall speed, V_{stall}. The rotational distance is the total distance covered in two seconds, which allows the pilot to make any adjustments to control surfaces and verify instruments, before starting to climb. The last segment, transitional distance, is the necessary distance to be able to fly over the 50ft obstacle to satisfy the FAA requirement. Last, the climbing angle was computed using geometry, and it is the relationship between the aircraft's rate of climb and takeoff velocity. Adding all the segments, the total distance needed for takeoff is 1803.74 feet which is well within the 2500 ft imposed by the RFP.

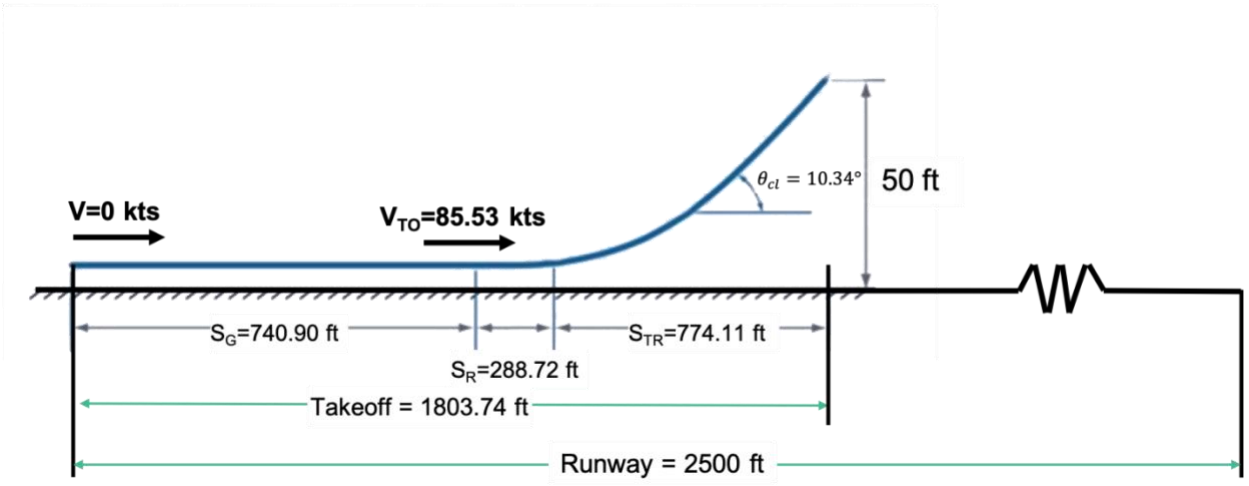

Figure 4.3-1 Takeoff segments and performance parameters

Similar to takeoff, the landing performance analysis was broken into its three main segments, as seen in Figure 4.3-2: air distance (S_A), free roll distance (S_{FR}), and braking distance (S_B). However, a new V_{stall} was calculated for this segment, as the aircraft weight and half of fuel remaining was

assumed to be an adequate weight for landing calculations. The landing distance begins from the point the aircraft is above a 50 ft high obstacle, per FAA requirement, and until the aircraft reaches a complete stop. The air distance is a function of lift over drag and the velocity with which the aircraft flies over the 50 ft obstacle. Furthermore, by the time the aircraft reaches a velocity that is $1.15V_{Stall}$, touchdown velocity (V_{TD}), the airplane will cover the free roll distance in about 3 seconds, where the pilot will retract the flaps and throttle down the power to idle. The remaining segment is the distance the airplane will need to come to a complete stop. After calculating the distances for the three main segments, the airplane needs a total distance of about 1411 ft, which is within the 2500 ft runway requirement that was stated by the RFP.

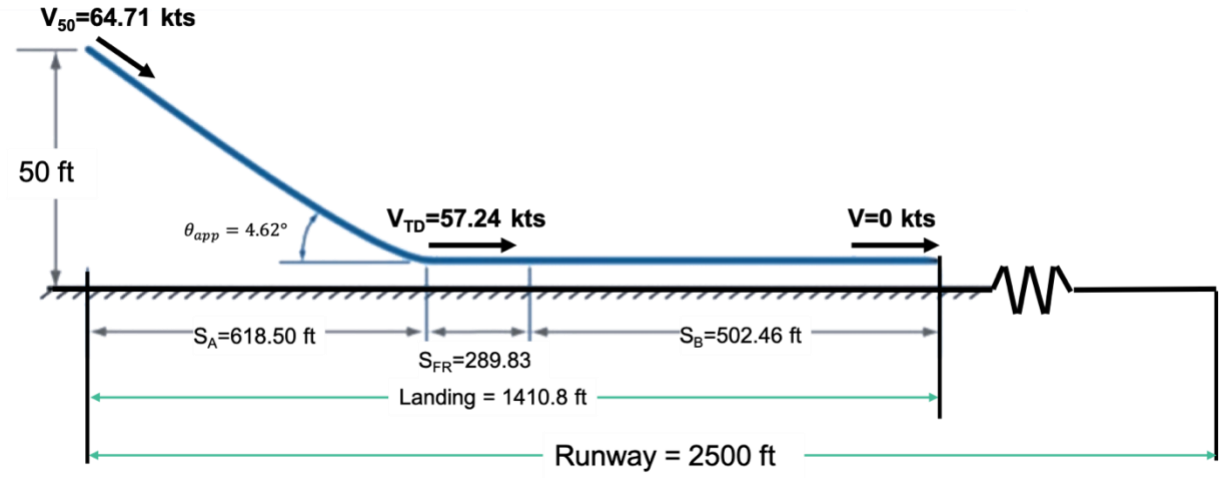

Figure 4.3-2 Landing segments and performance parameters

Since the Envoy 600 is a dual engine aircraft, a balanced field length was calculated to determine if the airplane would be able to continue with the takeoff if one engine were to become inoperable or come to a complete stop with the given runway length. This is shown in Figure 4.3.3. During takeoff, if the engine fails before 49.2 kts, the pilot would have at least 3 seconds before reaching the decision velocity, V_1 = 65.9 kts. In either case, the Envoy 600's balanced field length is

achievable within the 2500 ft runway, as it can completely stop or continue takeoff within a length of about 1400 ft.

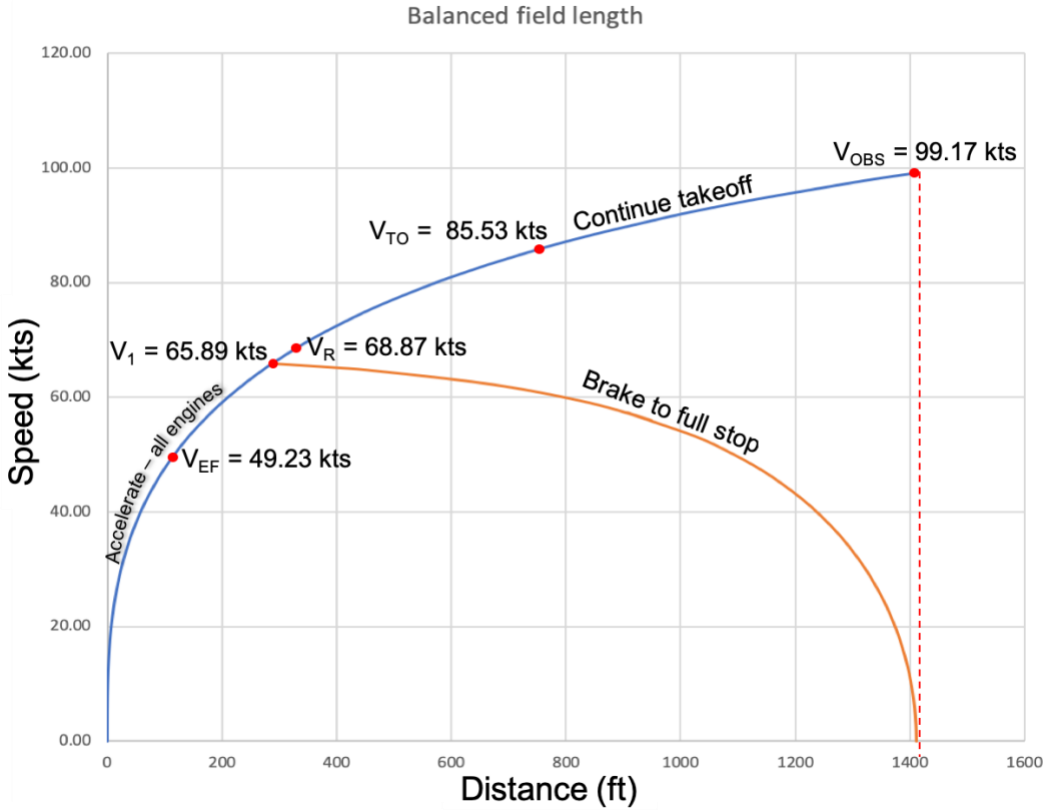

Figure 4.3-3 Balance field graph of speed vs distance

4.4 Climb Performance & Flight Envelope

The RFP did not state a rate of climb requirement, so the chosen rate of climb was based off the minimum FAR requirement of 300 fpm. Analysis was conducted for lowering the fuel burn and meeting the mission requirements for time and average ground speed. The resulting climb performances can be seen in table 4.4-1.

Table 4-3 Climb Performance

Segment	Speed (kts)	Rate of Climb (fpm)	Time (min)
Climb 1	100	1984	4.03
Climb 2	100	1281	2.34

The Envoy 600 operating envelope was found by determining the lowest possible level flight speed, which is equivalent to the aircraft stall speed, and the maximum speed achieved at full power. As shown in Figure 4.4-1 these two intersect at a ceiling altitude of 28000 ft. However, to prevent the need for cabin pressurization, we limited our aircraft operations to below 12,500 ft. Thus, having a cruise design point at 8000 ft at a speed of 206 kt.

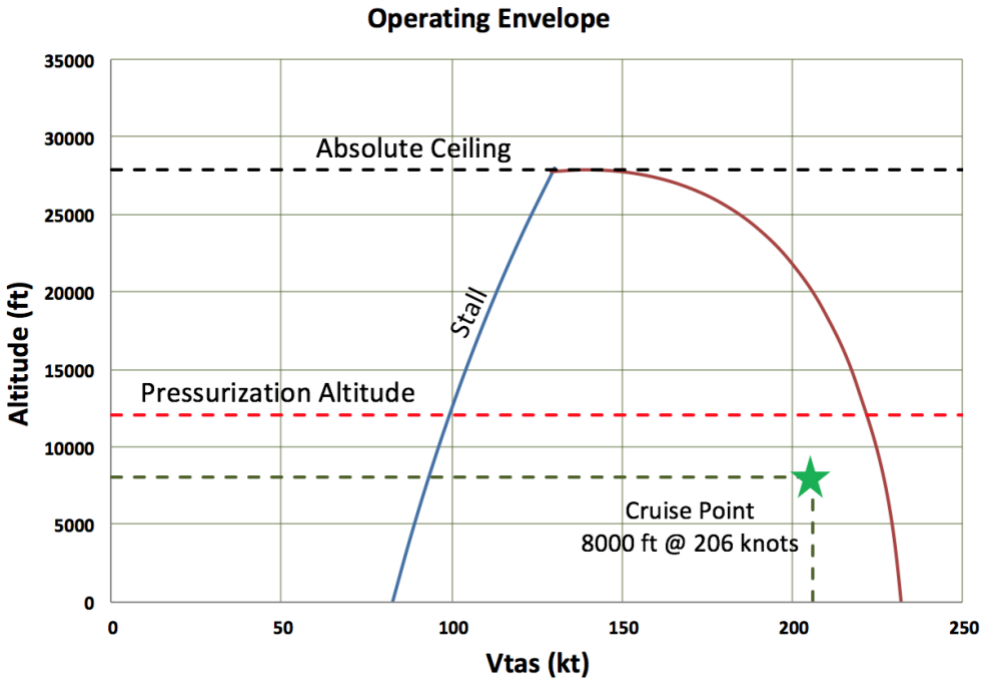

Figure 4.4-1 Operating Envelope

4.5 Range Performance

The payload range is an indicator of how far the aircraft will fly given the amount of payload and fuel it can carry. The RFP states requirements for the sizing mission such as the load and total range. For this mission, the aircraft must carry full payload and have a minimum range of 250 nautical miles. As shown in Figure 4.5-1, based on our mission calculations we achieved the minimum range. The Figure also shows that the reference mission is well within the boundaries of our payload-range capacity. While not a requirement, in the event the aircraft needs to be ferried, it is capable of a range of just under 350 nmi with no payload.

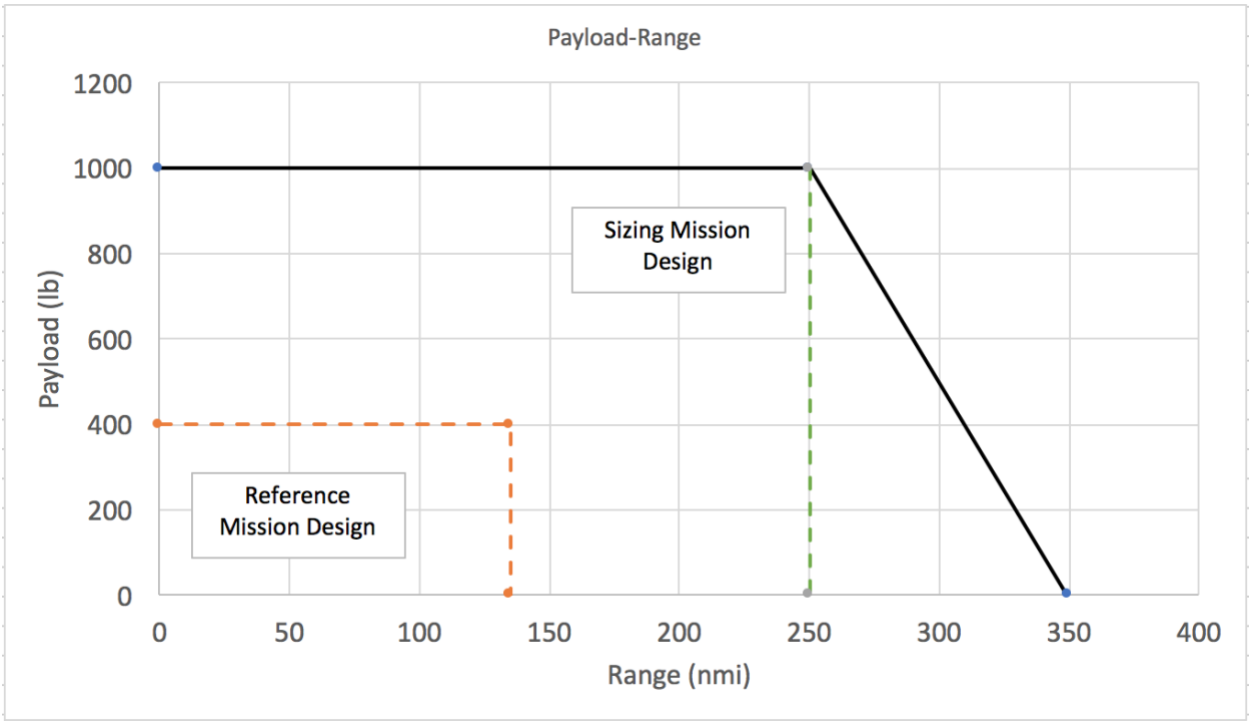

Figure 4.5-1 Payload-Range Chart

Loiter velocity was found in MATLAB by and calculating the power required for a given velocity at an altitude of 3,000 ft and finding minimum power required as shown in Figure 4.5-2. With the magenta dot representing the best loiter speed of 86.45 kts requiring 85.20 horsepower.

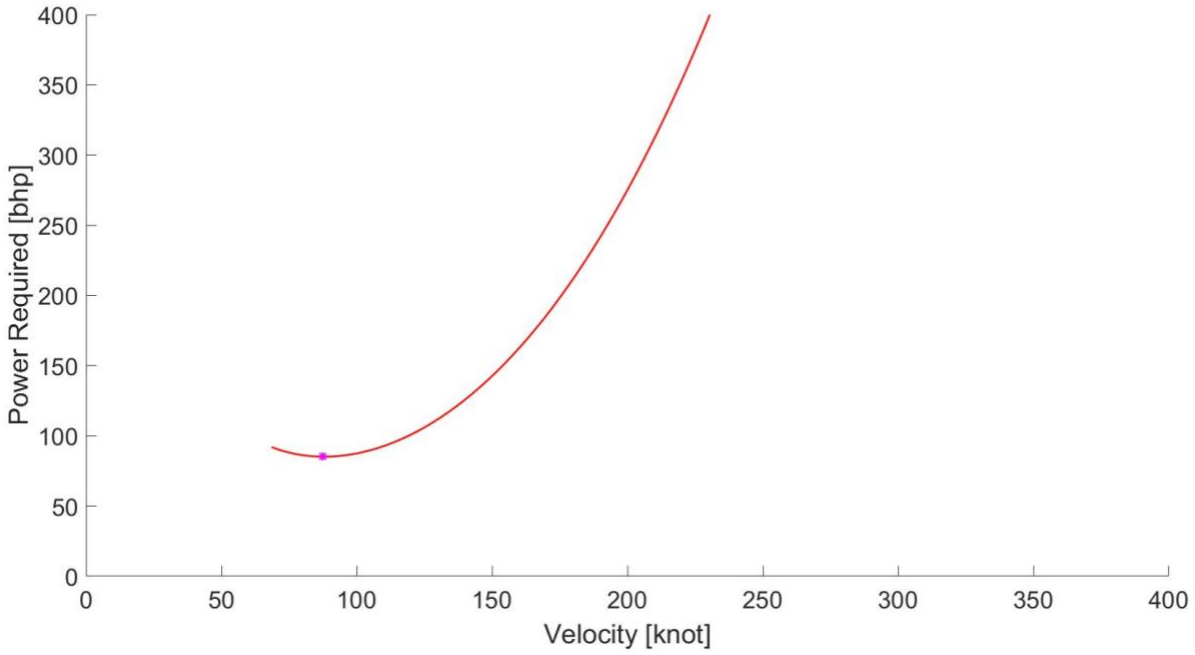

Figure 4.5-2 Power Required vs Velocity

4.6 Trade Study: Cruise Velocity and Altitude

Since the RFP did not specify cruise conditions, the optimum cruise velocity and altitude needed to be determined. The selection of cruise speed and altitude was based off the reference mission as it has a time constraint. The resulting cruise condition was also used for the sizing mission. Varying cruise velocity and altitude to evaluate the fuel needed, a carpet plot of fuel burned vs combinations of velocity and altitude was generated. The altitude was varied from 3000 feet to 10,000 feet, as going above 10,000-12,000 feet would require cabin pressurization. The constraints include maximum 45 minutes for segments 3-5 (from RFP) and engine efficiency at various altitudes. The main deciding factor was the amount of fuel burned. The carpet plot generated is shown in Fig. 4.6-1.

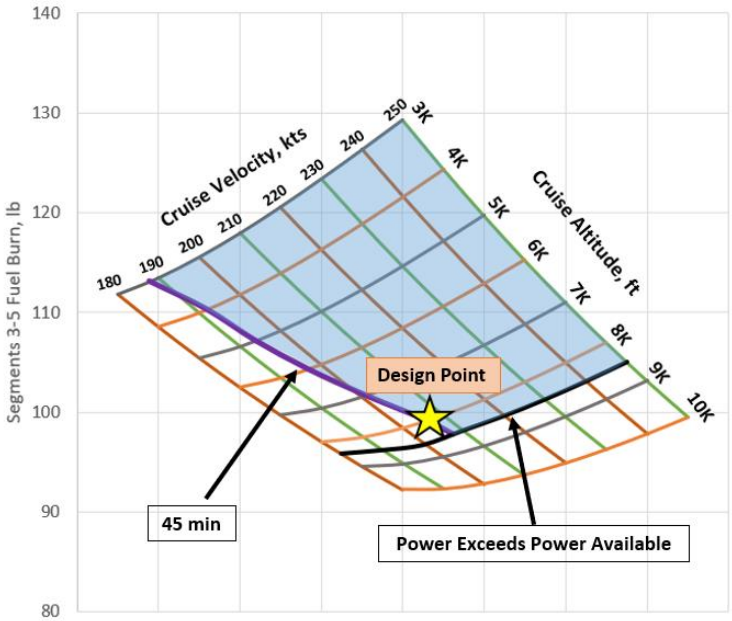

Figure 4.6-1 Cruise Conditions Trade Study

As expected, at higher cruise altitudes less fuel is burned. However, due to engine power decreasing at higher altitudes, the altitude could not exceed 8500 feet based on our mission analysis. As fuel burned was the main decision factor of the design space, the cruise condition was chosen to be 8000 feet at 206 knots. This allows the aircraft to operate with less fuel while still meeting the range, time and average ground speed requirements.

4.7 One Engine Inoperative Climb

FAA regulations require a climb gradient of 1.5% in case of a critical engine failure while exceeding 1.2 V^{S1} (takeoff stall speed) at 5,000 ft pressure altitude. This requirement was evaluated by calculating the aircraft at its takeoff conditions in 5,000 ft pressure altitude, with one engine at maximum continuous power. The calculated climb gradient was 7.9%, which exceeds the climb gradient required by the FAA. Thus, the aircraft is able to meet one engine inoperative climb requirements.

4.8 Engine Noise Limitations

According to 14 CFR Appendix G 36.301 Subsection C,

"...the noise level must not exceed 70dB(A) for aircraft having a maximum certificated takeoff weight of 1,257 pounds (570 kg) or less. For aircraft weights greater than 1,257 pounds, the noise limit increases from that point with the logarithm of airplane weight at the rate of 10.75dB(A) per doubling of weight, until the limit of 85dB(A) is reached..."

With our maximum takeoff weight of 3434 lb, the noise must not exceed 85 dB limit. Since our aircraft is still in the conceptual phase of design, we used comparable aircraft data to estimate our aircraft noise levels. We looked at two comparable aircraft, the Kings Engineering Model 44 and Partenavia P68 Observer 2. The Model 44 has twin Lycoming IO 540-M1A5 engines rated at 300 horsepower each and a maximum takeoff weight of 5800 lbs. The P68 is a twin IO-360-A1B6 rated at 200 horsepower each and a maximum takeoff weight of 4600 lb. According to Noise Level Data published on the FAA website, the Kings Engineering 44 has an estimated noise level at 84.2 dB while the P68 has an estimated noise level of 78.2 dB. With our weight lower than the P68 and having the same type of engines we estimate that our aircraft will have a noise level range of 76 – 80 dB which is under the maximum requirement.

Table 4-4 Estimated Aircraft Noise Levels

Aircraft	Noise Level (dB)	Compliance
Kings Engineering Model 44	84.2	Yes
Partenavia P68 Observer 2	78.2	Yes
Envoy 600	76 - 80	Yes

5 AERODYNAMICS

5.1 Airfoil Selection

Selection criteria for the airfoil is to have low drag, acceptable thickness ratio for structural and fuel volume considerations and high lift coefficient. Airfoils that were considered were the NACA 1412, 2412, 4412, 23012 and 23015. 6-series airfoils were considered but due to prop wash flow over the wing, laminar flow would be lost, thus not worthwhile. Table 5-1 displays the criteria that was used to select the chosen airfoil.

Table 5-1 Comparison of NACA 1412, 2412, 4412, 23012, and 23015 airfoils performance

NACA	**1412**	**2412**	**4412**	**23012**	**23015**
$C_{L\ cruise}$	0.265				
$C_{D\ cruise}$	0.0340	0.0340	0.0341	0.0339	0.0345
$C_L/C_{D\ cruise}$	7.793	7.799	7.7617	7.821	7.672
$C_L/C_{D\ max}$	11.769	11.827	11.986	11.952	11.835
C_L at $C_L/C_{D\ max}$	0.7	0.7	0.72	0.7	0.7
Horsepower required (hp)	268.81	268.59	269.89	267.86	273.06
$C_{L\ max}$	1.42	1.51	1.50	1.61	1.55

Reason for such similarity is because inviscid drag due to lift is greater than viscid drag due to lift, which is why the difference in horsepower required is a small value. Therefore, the airfoil with the highest C_{Lmax} was chosen: NACA 23012, as it will require lower flap deflection for takeoff and landing, and required the least horsepower needed at cruise. Figure 5.1-1 shows the cross section of NACA 23012 airfoil showing max camber location and max thickness location.

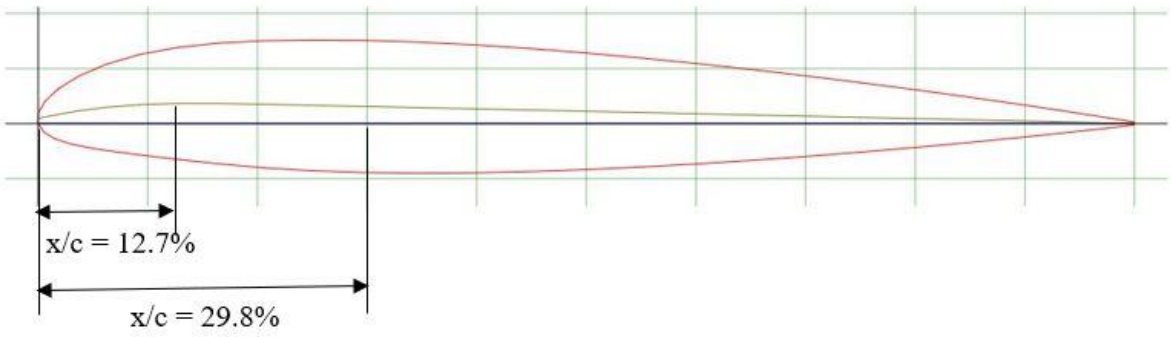

Figure 5.1-1 NACA 23012 Airfoil Cross Section

5.2 Wing Geometry

Wing planform was selected to be a straight tapered wing because maximum speed is below Mach divergence. Therefore, there is no reason to sweep the wing for aerodynamic purposes. Swept wings tend to also be heavier. The planform area was determined from the MTOW of 3,434 lb_f and wing loading of 31 psf from the constraint diagram to be 110.8 ft^2.

The taper ratio was determined using a vortex lattice program called XFLR5. Using a wing model with the area and aspect ratio being constant and varying the taper ratio from 1 to 0.357, as 0.357 being the optimum choice for reducing lift induced drag. A taper ratio of 0.5 is shown to be the best, shown in Figure 5.2-1 and Figure 5.2-2. The reason for this was to optimize both weight and drag of the wing for a given aspect ratio. In Figure 5.2-1 and Figure 5.2-2, the lift curves for taper ratio of 0.357 were not labeled because both lift curve for taper ratio of 0.5 and 0.357 are on top of each other; hence, both lines for a given aspect ratio can be considered the same line. The wing planform is shown in Figure 5.2-3 with Table 5.2-1 showing parameter values of the wing.

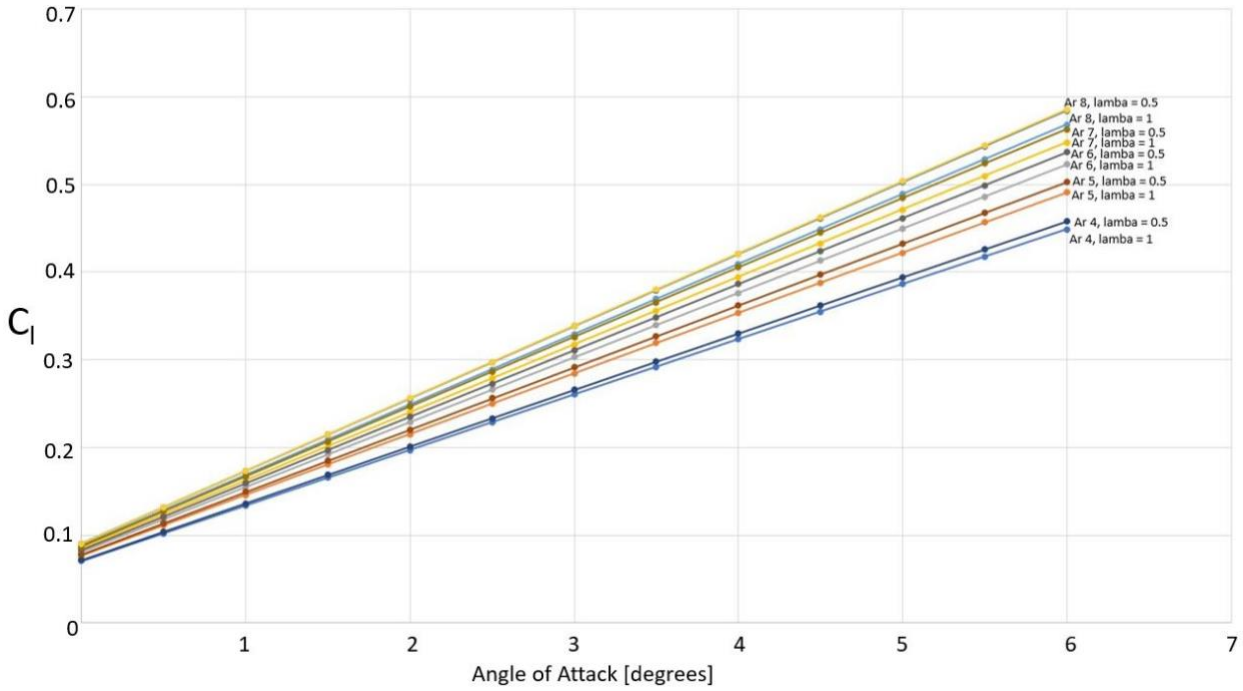

Figure 5.2-1 Lift Curve Slope Varying with Aspect Ratio and Taper Ratio

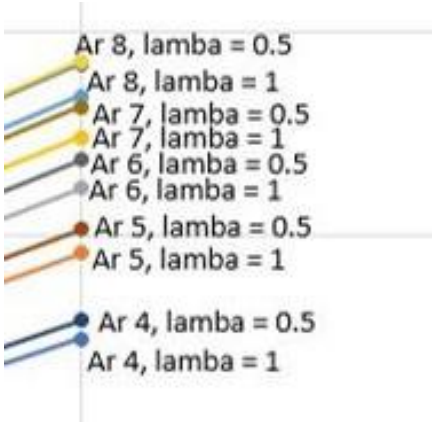

Figure 5.2-2 Zoomed in Lift Curve Slope Varying with Aspect Ratio and Taper Ratio

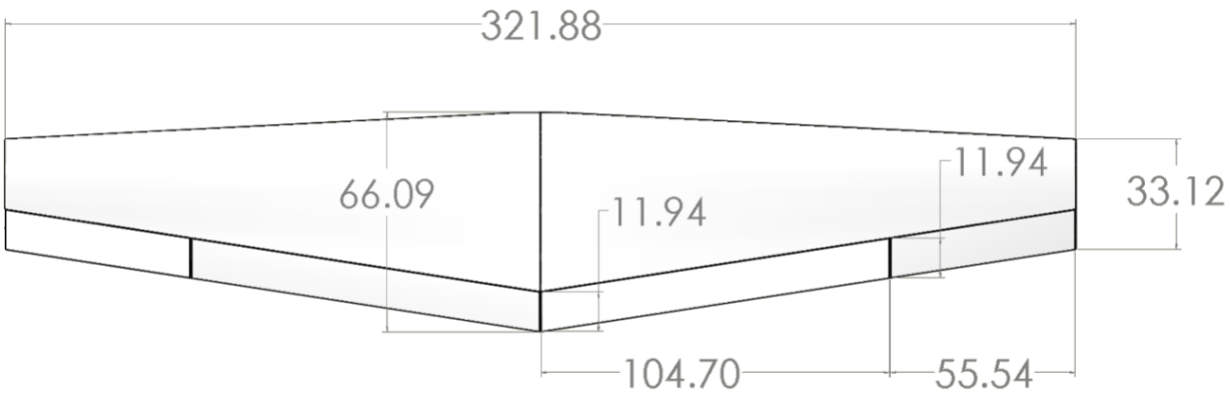

Figure 5.2-3 Wing Planform

Table 5-2 Wing Geometric Parameters

Parameter	Value
Planform Area, S [ft^2]	110.77
Wetted Area, S_{wet} [ft^2]	204.17
Leading Edge Sweep, Λ_{LE} [degree]	2.94
Trailing Edge Sweep, Λ_{TE} [degree]	-8.75
Span, b [ft]	26.83
Root Chord, c_r [ft]	5.50
Tip Chord, c_t [ft]	2.75
Mean Aerodynamic, Chord MAC [ft]	4.28
Wing Loading, $\frac{W}{S}$ [$\frac{lb_f}{ft^2}$]	31

5.2.1 Trade Study: Aspect Ratio and Takeoff Weight

After selecting a wing planform, a trade study was conducted to find the best aspect ratio for the aircrafts mission. A plot of varying aspect ratios vs wing loading was created including lines of constant overall aircraft weight. The two constraints that drove the design point were: a vertical constraint of the previously chosen wing loading at 31 psf and a horizontal constraint that represents the lowest possible aspect ratio at which the reference mission can be performed within the allowed 45 minutes. Through this method, we noted that as aspect ratio increased, so did the overall weight. With these constraints, as shown in Figure 5.2.1-1, we determined the best wing aspect ratio to be at 6.5 which is equivalent with the lowest overall aircraft weight.

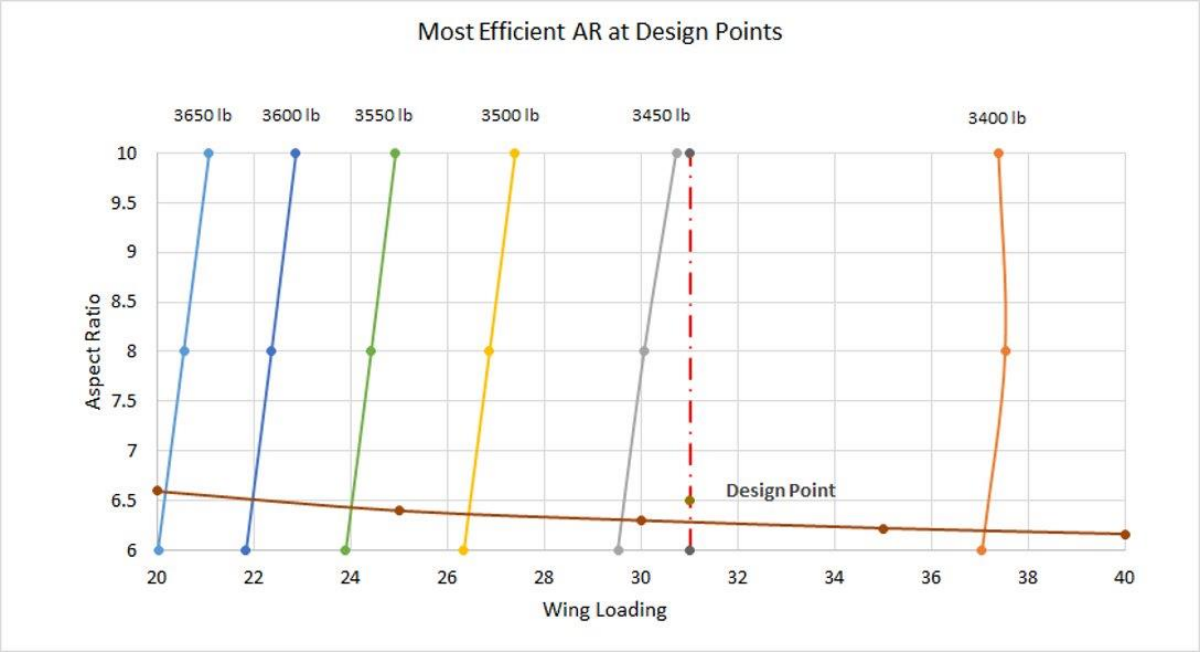

Figure 5.3 Aspect ratio and takeoff weight trade study

5.3 Flap Design

To meet the takeoff and landing requirement a C_L of 1.8 or greater is required. A plain flap was chosen since the C_L increment need is below 0.3 and is the simplest and cheapest option. Each flap has a span of 5.96 ft., with $c_f/c = 0.2$, with the area of each flap is 5.06 ft^2. Figure 5.3-1 and Table 5.3-1 show the flap deflection, angle of attack and coeffienct of lift for takeoff, cruise and landing.

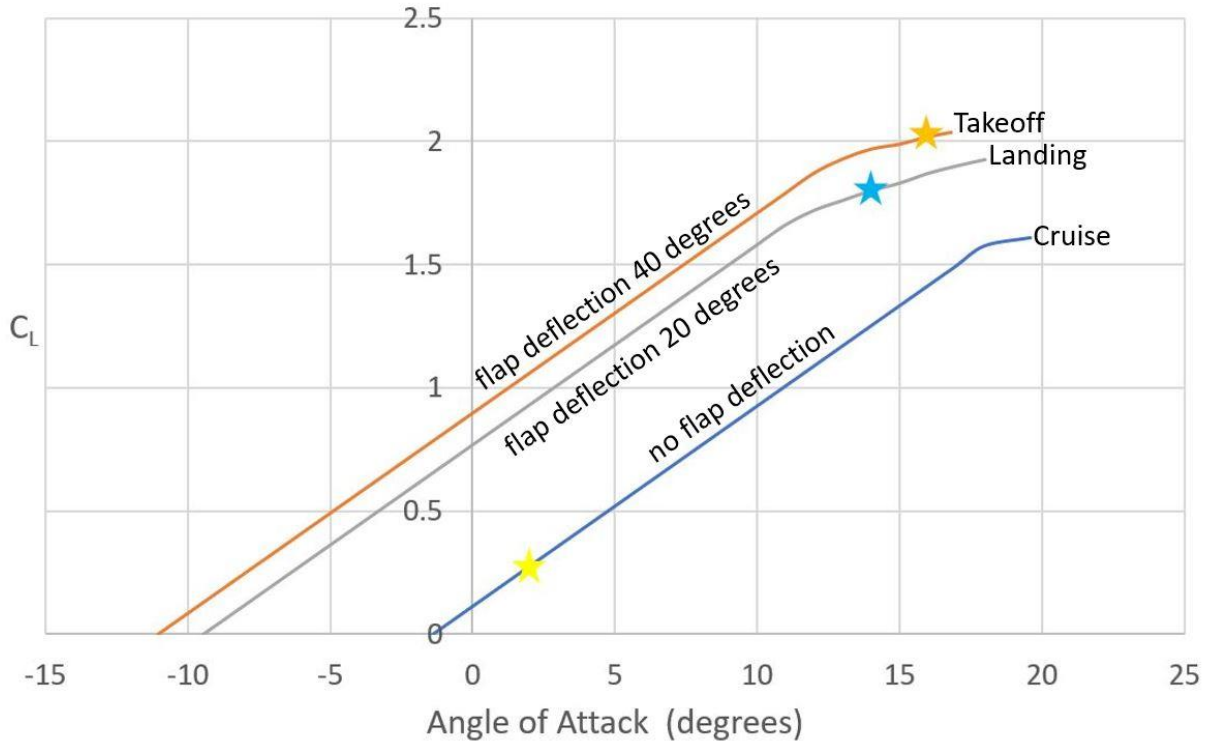

Figure 5.3-1 Lift Curve Slope versus flap deflection

Table 5-3 Coefficient of Lift, Alpha and Flap Deflection for Takeoff, Cruise and Landing

	C_L	α (degrees)	δ (degrees)
Takeoff	2.02	16	40
Cruise	0.273	1.96	0
Landing	1.80	14	20

5.4 Lift & Drag Models

The Drag Buildup for parasite drag for fuselage, wing, horizontal tail, vertical tail, engine nacelles and fixed gear was generated in MATLAB. For fixed gear, parasite drag was set to be a constant 0.006 using data from Nicolai and Carichner [5]. Surface areas were found using OpenVSP. Our will be cruising at a Reynold number of 8.98×10^6, therefore it is assumed that all components are fully turbulent. Figure 5.4-1 and Table 5.4-1 display the drag breakdown of the aircraft, with Figure 5.4-2 and Table 5-4 displays the wetted surface area for each component.

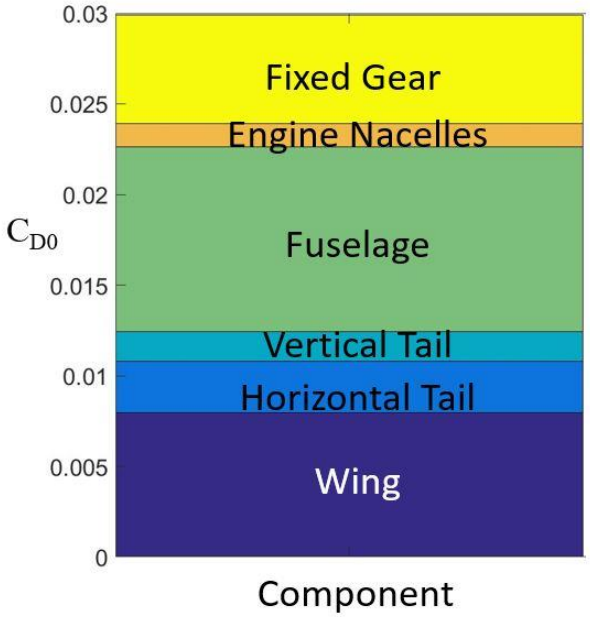

Figure 5.4-1 Drag Buildup of Parasite Drag Coefficient of each Component at Cruise

Table 5-4 Parasite Drag Coefficient Numbers of each Component at Cruise

Component	Parasite Drag Coefficient	Percentage of Total Parasite Drag
Wing	0.00796	26.62
Horizontal Tail	0.00283	9.46
Vertical Tail	0.00163	5.44
Fuselage	0.0102	34.19
Nacelles	0.00126	4.22
Fixed Gear with Fairings	0.0060	20.07
Total	0.0299	100

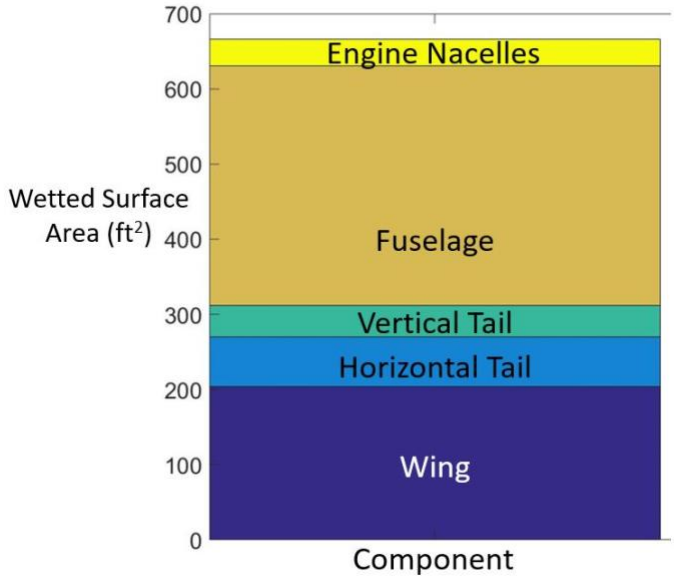

Figure 5.4-2 Wetted Surface Area of each Component

Table 5-5 Wetted Surface Area Numbers of each Component

Component	**Wetted Surface Area (ft^2)**	**Percentage of Total Wetted Surface Area**
Wing	204.14	30.67
Horizontal Tail	66.37	9.969
Vertical Tail	41.02	6.161
Fuselage	318.67	47.87
Nacelles	35.52	5.336
Total	665.76	100

The total parasite drag coefficient was calculated in MATLAB and cross-checked with OpenVSP parasite drag calculator for the same altitude using Standard Day conditions and velocity. Drag polar was generated up to C_{Lmax} for each segment, after correcting for downwash effects for landing. Drag polar for takeoff, cruise and landing are shown in Figure 5.4-3 and the range factor ($\frac{C_L}{C_D}$) in Figure 5.4-4.

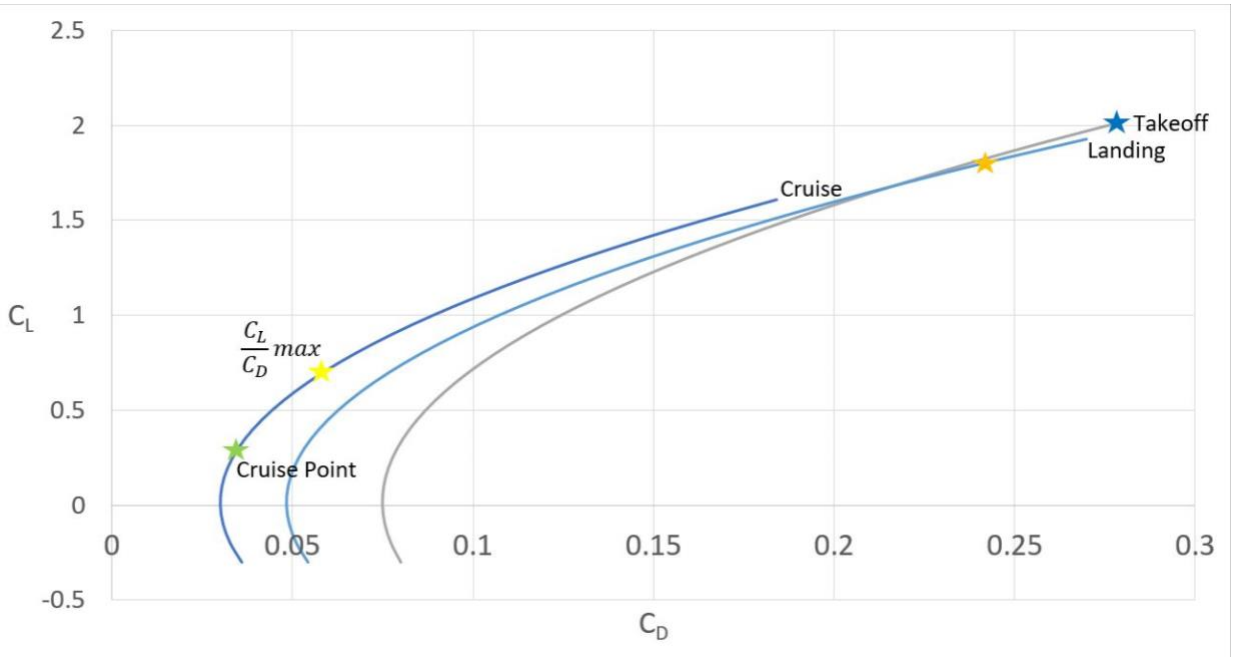

Figure 5.4-3 Drag Polar for Takeoff, Cruise and Landing.

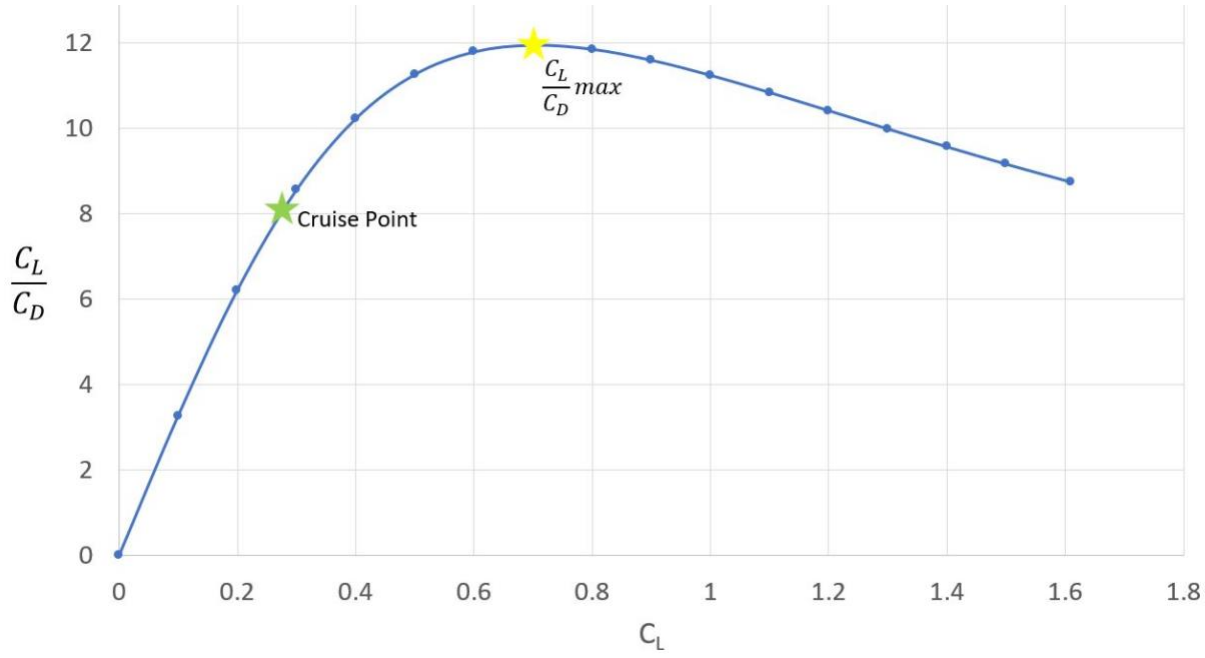

Figure 5.4-4 L/D vs Coefficient of Lift

As shown above the cruise conditions and conditions for $\frac{C_L}{C_{D_{max}}}$ are far apart, for cruise condition C_L = 0.0273 and $\frac{C_L}{C_D}$ = 7.99 while $\frac{C_L}{C_{D_{max}}}$ = 11.9 at C_L = 0.70. The time requirement for cruise

conflicted with being able to fly at $\frac{C_L}{C_{D_{max}}}$. It is achievable to fly at $\frac{C_L}{C_{D_{max}}}$ at higher altitude, but this will require pressurization and more power because of the higher speed.

6 PROPULSION

6.1 Engine Requirements

To ensure that all requirements of the propulsion systems are met, the requirements are outlined below in Table 6-1.

Table 6-1 Engine Requirement

Description	Requirement	Source
Horsepower Requirement	378 HP	Constraint Diagram
Single Engine Requirement	If single engine, fuselage parachute required	Request for Proposal

6.2 Engine Selection Process

Engine selection was performed via a series of trade studies to ensure that optimal engine architecture and engine is selected. The engine trade studies were accomplished via preliminary analysis, as further design and analysis of the aircraft was not possible without a chosen engine.

6.2.1 Electric Propulsion Analysis

Before a broad trade study for propulsion architecture selection, viability of electric propulsion system was analyzed. The electric aircraft's properties used for analysis are shown below in Table 6-2.

Table 6-2 Properties Used for Electric Aircraft Analysis

Aircraft Empty Weight	2075 lb
Aircraft Cruise Speed	160 kt
η_{prop}	0.85
Number of Discharges	1040
Depth of Discharge	90%
Estimated Wire Length	20m

For electric propulsion, Twin EMRAX 268 was chosen as it was the only electric aircraft engine available that met the power requirement. The specifications of EMRAX 268 is shown below in Table 6-3 [11].

Table 6-3 EMRAX 268 Specifications

Operating Voltage (DC volts)	680
Weight (lb)	43.9
Peak Power (hp)	308.4
Continuous Power (hp)	54-107
Max Current (Amps)	400
Continuous Current (Amps)	190
Efficiency (%)	92-98

The battery used was Kokam SLPB080085270 UHC NMC cells, the cells possessed the highest energy density that was found in commercial battery cells. The cell's specifications are shown in Table 5.2.1-3 [12].

Table 6-4 Kokam UHC NMC Battery Cell Specifications

Capacity (Ah)	Dimension (mm)			Weight (kg)	Discharge Rate		Energy Density (Wh/kg)
	W	L	T		C-rate(C)		
					Continuous	Pulse	
27	95	272	7.8	0.38	2	4	260

For the analysis, factors such as cell volume, cell energy density, cell weight, capacity fading, depth of discharge, number of discharge cycles, delivery loss, battery redundancy, and electronic speed controller's mass was factored. With the properties of the system, the electrical propulsion

system was iterated until it was able to meet the mission requirements. The resulting electric propulsion system's specifications are shown below in Table 6-5.

Table 6-5 Electric Propulsion System Specifications

Battery Mass	1385 lb
Battery Volume	11.53 ft^3
Total Mounted System Mass	804 kg
Battery Capacity	378 Ah
Battery Energy	163.4 kWh
Charging Time from 90% (40A Charging)	9.1 hr

As shown, the charging time required to fly was exceedingly high, and was unable to meet the mission requirements of 20 flights per week. In addition, the required overhaul cost required for the system far dwarfs the estimated direct operating cost savings compared to the internal combustion system resulting in a far higher annual cost, as shown in Figure 6.2.1-1.

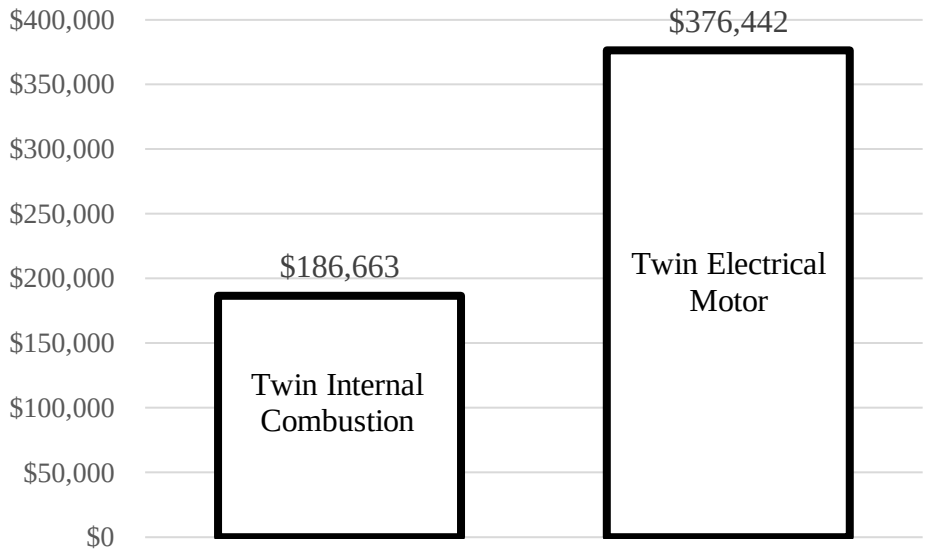

Figure 6.2.1-1 Annual Cost Comparison Between Internal Combustion and Electrical Propulsion

Thus, the electric configuration was eliminated from further design.

6.2.2 Propulsion Architecture Selection

In order to select propulsion architectures, representative propulsion systems were selected to be analyzed and compared against. Each propulsion system was analyzed and graded for a set of figures of merit, weighted to emphasize reduction of direct operating cost and operating efficiency. The representative propulsion system is as follows. For single engine internal combustion propulsion, PT6A-25 turboprop engine was chosen. For multi-engine internal combustion propulsion system, twin Lycoming IO-360-A1A engines was chosen. The performances of the candidate engines are shown in Table 6-6.

Table 6-6 Performance of Propulsion System Candidates

Total Performance Metric	PT6A-25	Twin Lycoming IO-360-A1A
Brake Specific Fuel Consumption at Cruise (lb/hr/hp)	0.63	0.41
Total Purchase Cost	$500,000	$116,000
Total Overhaul Cost	$200,000	$48,000
Installed Weight (lb) (Dry weight*1.15 if unavailable)	377	674
Overhaul Cycle (Hr)	3600	2000

The figures of merit are shown on Table 6-7. The figures of merit are ranked from 1 to 5, where 5 indicates the good performance for the figure of merit, while 1 indicates lacking performance.

Table 6-7 Figures of Merit for Propulsion Architecture Selection

Weighting Factor	SCORES:	1	2	3	4	5
0.15	Installation Weight (lb) (Dry weight*1.15 if unavailable)	800+	600 ~800	400 ~600	200 ~400	0~200
0.05	Price ($USD)	400k+	300k ~400k	200k ~300k	100k ~200k	0~100k
0.2	Fuel Weight Required (lb/Hr in Max Required Power)	200+	150 ~200	100 ~150	50 ~100	0~50
0.3	DOC ($/Hr Cruise)	220 ~260	180 ~220	140 ~180	100 ~140	0~100
0.05	Overhaul Cycle (Op. Hr)	0 ~500	500 ~1500	1500 ~2500	2500 ~3500	3500+
0.1	Does not need a Parachute	No		Yes		

The trade study is shown on Table 6-8 below.

Table 6-8 Propulsion Architecture Trade Study

Weighting Factor	Engines Figure of Merit	PT6A-25	IO-360-A1A (Twin)
0.15	Installation Weight (lb)	4 377	2 674
0.05	Price ($USD)	1 $500,000	4 $116,000
0.2	Fuel Weight Required (lb/Hr in Max Required Power)	1 209.76	3 141.9
0.3	DOC ($/Hr Cruise)	3 143.6	4 117.7
0.05	Overhaul Cycle (Op. Hr)	5 3600	3 2000
0.1	Does not need a Parachute	1	3
0.15	Fuel weight is consumed	3	3
1	Weighted Total	2.75	3.2

From this trade study, it was determined that twin internal combustion engine was the better propulsion architecture choice compared to a single turboprop engine.

6.3 Final Engine Selection

As shown though the trade study above, the twin internal combustion engine was chosen to be the most efficient propulsion architecture. To select the most suitable engine for this architecture, another trade study between two engines were compared. For this comparison, the smallest engines that meet the requirements were considered, as excess power above the requirement was deemed

to result in excess costs and weight. While there are numerous engines that fit the requirements under the twin engine propulsion architecture, many are simple variations of the same engine, and thus offer negligible performance differences.

The selection lead to two engines that met the power requirements: the Lycoming IO-360-A1A and Continental IO-360-ES. Their respective performance specifications are shown below in Table 6-9.

Table 6-9 Performance Specifications of Engine Candidates

Total Performance Metric	Twin Lycoming IO-360-A1A	Twin Continental IO-360-ES
Brake Specific Fuel Consumption at Cruise (lb/hr/hp)	0.41	0.63
Total Purchase Cost	$116,000	$500,000
Total Overhaul Cost	$48,000	$200,000
Installed Weight (lb) (Dry weight*1.15 if unavailable)	674	377
Overhaul Cycle (Hr)	2000	3600

These choices were evaluated using a trade study, similar to the propulsion architecture trade study conducted previously. Again, figures of merits that impact direct operating cost were prioritized by the weighting factor. The figures of merit are shown below in Table 6-10.

Table 6-10 Figures of Merit for Final Engine Selection

Weighting Factor	SCORES:	1	2	3	4	5
0.25	Installation Weight (lb)	700+	690~700	680~690	670~680	0~670
0.1	Purchase Price ($)	120k+	110k~120k	9k~110k	80k~90k	0~80k
0.2	Fuel Weight Required (lb. required/Hr in Max Required Power)	148+	146~148	145~146	143~145	0~142
0.3	DOC ($/Hr Cruise)	130+	120~130	110~120	100~110	0~100
0.15	Overhaul Cost ($USD)	20500+	19500~20499	18500~19499	17500~18499	0~17499

The trade study of the engine is shown in Table 6-11.

Table 6.2.3-1 Trade Study of Final Engine Selection

Weighting Factor	Engine Figures of Merit	Lycoming IO-360-A1A	Continental IO-360-ES
0.25	Installation Weight (lb)	4 674	1 702
0.1	Purchase Price ($USD)	2 $116,000	4 $88,000
0.2	Fuel Weight Required (lb. required/Hr in Max Required Power)	5 141.45	4 144.9
0.3	DOC ($/Hr Cruise)	3 117.7	3 120.5
0.15	Overhaul Cost ($USD)	3 $19,295	1 $25,265

1	Weighted TOTAL	3.55	2.5

As shown, the final engine chosen is the Lycoming IO-360-A1A.

6.3.1 Fuel System Overview

To facilitate the multi-engine propulsion system, each engine is fitted with its own fuel pump to feed itself fuel. In addition, the fuel tanks on each wing are outfitted with fuel pumps and cross valves to facilitate cross feeding and transfer of fuel across tanks. This will allow for adjustment of fuel levels in each wing, as well as feeding of fuel from both tanks in case of a single engine failure. To maximize volume usage and weight savings, the fuel tanks will be integrated into the wings. Therefore, the tanks are sealed compartments in the wings. The fuel being used is aviation gas and has a density of 1 US gal/lb. The calculated amount of fuel needed is about 236.8 lbs of fuel. Hence the volume taken up by the aviation gas is 5.27 ft^3. Since an integrated tank is being used the actual fuel volume is calculated by getting the fuel volume and dividing by a packing factor of 0.75. Therefore, the total volume for the fuel tank in the wing is about 7.03 ft^3.

6.3.2 Propulsion System Performance Overview

The final propulsion system's performance specifications are shown in Table 6-11.

Table 6-11 Propulsion System Performance Specifications

Performance Metric	Twin Lycoming IO-360-A1A
Brake Specific Fuel Consumption at Cruise (lb/hr/hp)	0.41
Total Purchase Cost	$116,000
Total Overhaul Cost	$48,000
Installed Weight (lb) (Dry weight*1.15 Estimation)	674
Overhaul Cycle (Hr)	2000
Maximum Continuous Power per Engine (HP)	200
Fuel Used	Aviation Gasoline

6.4 Propeller Selection

Propeller was selected on the history of usage on similar engines. For this, Pitts HC-C2YK-4AF propeller was chosen, as it was designed for usage on the IO-360-A1A. The relatively small 72" propeller diameter also was seen as a positive, as it allowed closer engine placement to the center of the aircraft, reducing moment generated in case of a single engine failure.

7 STABILITY & CONTROL

7.1 Empennage

7.1.1 Tail Configuration

A conventional configuration for the empennage requires less internal structures, and, thus, reduces the weight and cost of production while still providing adequate stability, trim and control for our aircraft. At the current operating speeds, the washout is very minimal. Thus, the horizontal stabilizer in the conventional configuration would not be highly impacted by washout effects and

did not present issues to consider any further calculations for a different horizontal stabilizer position.

7.1.2 Airfoil

Generally, airfoils for the horizontal and vertical stabilizers are for the most part symmetrical, so only airfoils with no camber were considered. Some of the most common airfoils for empennages that were found are NACA 0009 and NACA 0012. Also, as the thickness to chord ratio increases, usually, the lighter a wing gets, so we determined that the ideal point, before the drag increase becomes an issue, was at a thickness equal to 12% the chord. Thus, NACA 0012, Figure 7.1.2-1 below, was selected as the airfoil for both the vertical and horizontal stabilizer because it will produce enough negative lift from the horizontal stabilizer to make the aircraft naturally stable and it produces enough side force from the vertical stabilizer that will directionally stabilize the plane in case one engine becomes inoperable.

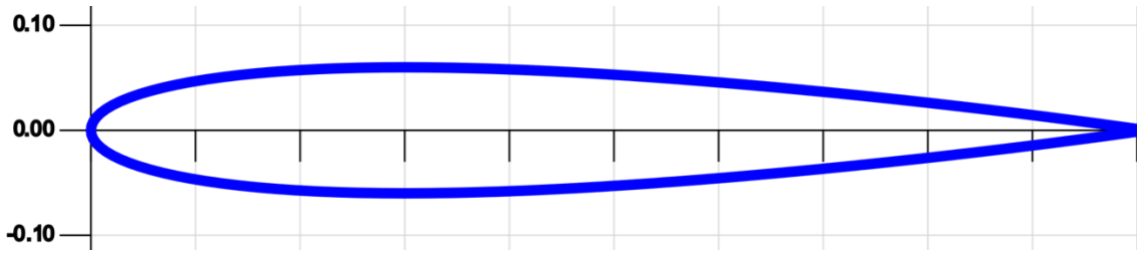

Figure 7.1-1 NACA 0012 Airfoil

7.1.3 Sizing

During the initial phases of the design of the Envoy 600, a tail volume coefficient approach was used to determine a preliminary size of the horizontal and vertical stabilizer. Volume coefficients for a two-engine propeller general aviation aircraft were taken from Nicolai and Carichner [5]. A $C_{HT} = 0.76$ and $C_{VT} = 0.06$ were used for the initial sizing of the empennage.

However, after further calculations and as the design of the aircraft progressed the values and size of the empennage were starting to be finalized, more detailed methods were used to obtain the minimum tail sizes.

For the horizontal stabilizer, values for rear stability, the nose wheel liftoff, and landing flare were calculated to construct a notch chart, Figure 5.4.3-1 below. Also, a center of gravity travel diagram was used to determine the range of how much the C.G. could move for different loading conditions. From the notch chart, the new horizontal tail volume coefficient, that provides adequate pitching stability to the aircraft, was determined to be $C_{HT} = 0.63$ as contrasted with the initial assumption of $C_{HT} = 0.76$.

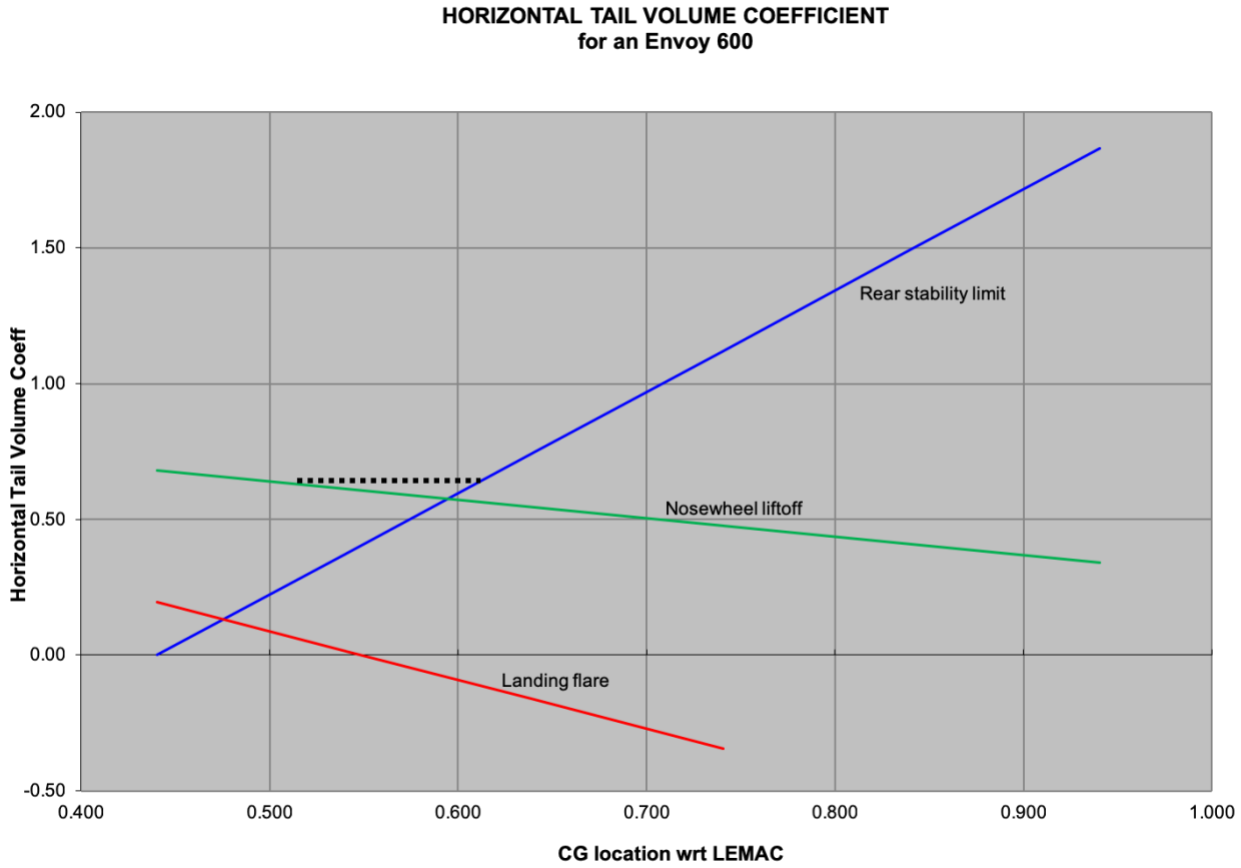

Figure 7.1-2 Horizontal Tail Volume Coefficient Notch Chart

In order to reduce the manufacturing costs of the horizontal tail, a taper ratio of 1 and no sweep was selected. Furthermore, using the obtained horizontal tail volume coefficient from the notch chart, the dimensions of the horizontal tail were calculated and are summarized in Table 7-1 below along with an engineering drawing of the horizontal tail can be seen in Figure 7-2.

Table 7-1 Horizontal Stabilizer Dimensions

Parameter	Symbol	Value
Horizontal tail volume coefficient	C_{HT}	0.63
Horizontal tail area	S_{HT}	31.16 ft^2
Span	b_{HT}	9.67 ft
Aspect Ratio	AR	3.0
Taper Ratio	λ	1.0
Leading Edge Sweep	Λ_{HT}	0°
Root Chord	$c_{r_{HT}}$	3.22 ft
Tip Chord	$c_{t_{HT}}$	3.22 ft
Mean Aerodynamic Chord	MAC_{HT}	3.22 ft

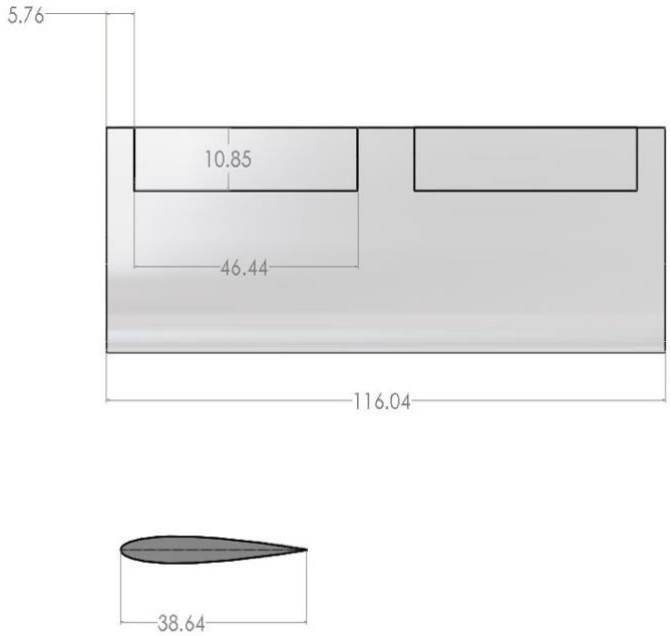

Figure 7.1-3 Horizontal Tail Drawing (inches)

Similar to the sizing of the horizontal stabilizer, another method was also needed to detail the size of the vertical tail. In order to determine the size of vertical tail needed to directionally stabilize the aircraft in case one engine becomes inoperable, a moment cancellation diagram was

constructed. The point where both the moment from the operating engine and the moment from the side force of the vertical tail are the same defines the minimum speed. This speed must be less than $1.1V_{stall}$, was determined to be the design point for sizing the vertical tail. As seen in Figure 7.1.3-3 below, a vertical tail size of 15.4 ft^2 produces enough side force to cancel out the moment produced by one engine at a velocity of 78.35 knots, which is less that the 1.1Vstall requirement, and thus will be used to calculate the geometry of the vertical stabilizer.

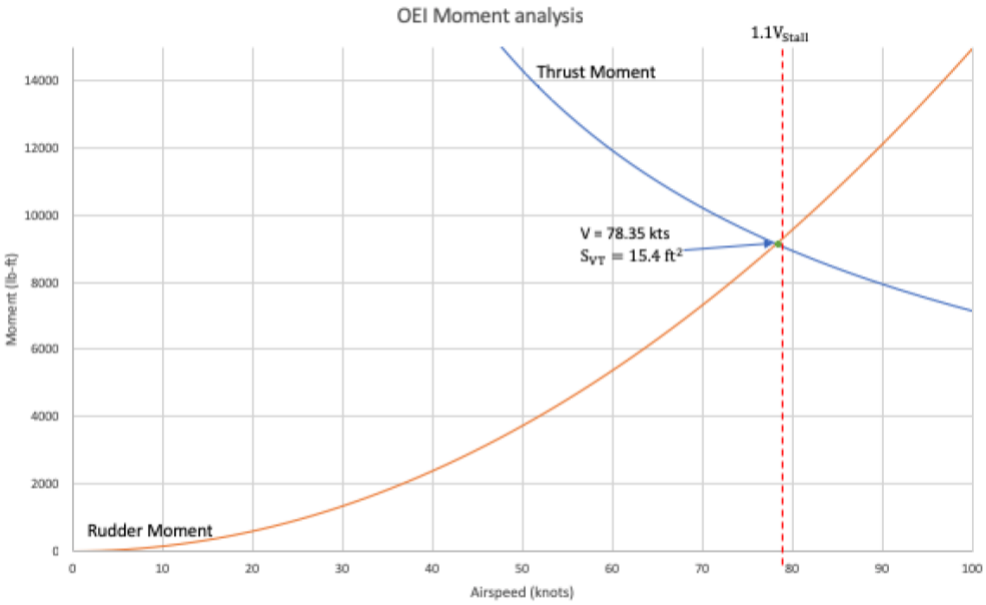

Figure 7.1-4 One engine inoperable moment cancellation diagram

The vertical stabilizers are used to reduce the side slip, to satisfy the longitudinal trim, and provide the necessary side force to keep the aircraft directionally stable. For airplanes that cruise at low speeds, the sweep angle of the vertical stabilizer is usually around 20°. Therefore, this parameter was used initially as a defining factor. Furthermore, during the estimation of the center of gravity of the aircraft, it was determined that the most favorable moment arm, for weight distribution, of the vertical stabilizer was at 10 ft aft of the CG, so, a sweep angle at quarter-chord of 21° was calculated and used, together with the area calculated in Figure 5.4.3-3 above, for the calculation

of the other dimensions of the vertical stabilizer. The dimensions of the vertical tail are summarized in Table 7-2 below along with an engineering drawing of the vertical, Figure 7.1.3-4.

Table 7-2 Vertical Stabilizer Dimensions

Parameter	Symbol	Value
Vertical tail volume coefficient	C_{VT}	0.048
Vertical tail area	S_{VT}	15.40 ft^2
Span	b_{VT}	4.47 ft
Aspect Ratio	AR	1.3
Taper Ratio	λ	0.6
Leading Edge Sweep	Λ_{VT}	21°
Root Chord	$c_{r_{VT}}$	4.30 ft
Tip Chord	$c_{t_{VT}}$	2.58 ft
Mean Aerodynamic Chord	MAC_{VT}	3.51 ft

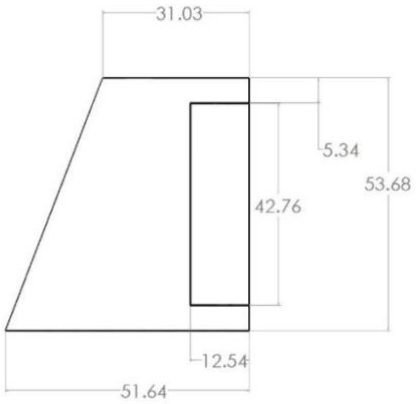

Figure 5.4.3-4: Vertical Tail Drawing (inches)

7.2 Control Surface Sizing

Control surface sizing was performed by calculating the control coefficients and comparing them to a similar aircraft, in order to ensure that the aircraft maintains maneuverability. Further detailed mass properties analysis of the aircraft would be required before handling quality analysis could be performed, so rudimentary comparison of control derivatives to a similar aircraft, Cessna 310, was deemed enough for the preliminary design phase.

For the main wing, $^{c_{control}}/_{c_{wing}} = 0.2$ was implemented for both flaps and ailerons. The dimensions are shown in Figure 7.2-1.

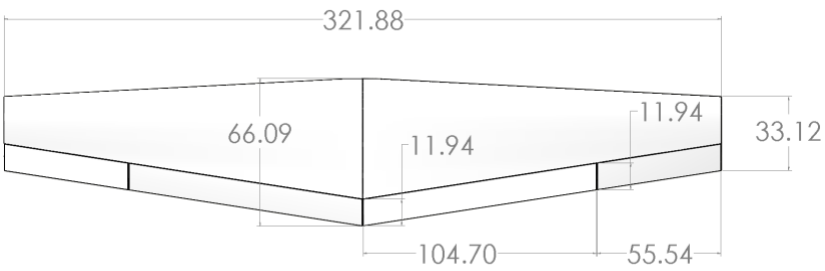

For the empennage, different control surface to chord ratio were considered and used to iterate calculation of key forces to design a stable aircraft. For the vertical stabilizer, the rudder chord to chord ratio affects the side force produced by the vertical stabilizer, and a ${}^{c_R}/_{c} = 0.3$ gave the most effective force to structural weight performance. Also, in order to reduce manufacturing costs, the design of the empennage control surfaces have a rectangular planform. Table 7-3 below summarizes the dimensions for the rudder and elevators.

Table 7-3 Rudder and Elevator dimensions, dimensions in ft.

	Chord	Span	Distance from the closest outer edge
Rudder	1.05	3.58	0.45
Elevator	0.97	3.87	0.48

Control derivatives bar the rudder control derivatives were determined using DATCOM. The Envoy 600 aircraft was recreated in Digital DATCOM and was analyzed for static and dynamic stability. Figure 7.2-2 shows a highly simplified drawing of the recreated aircraft in DATCOM.

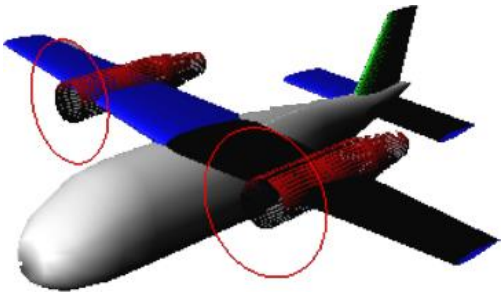

Figure 7.2-2 Envoy 600 in DIGIDAT

Table 7-4 shows the comparison of the determined control derivatives against a Cessna 310.

Table 7-4 Comparison of Control Derivatives

	Cessna 310	Envoy 600
$C_{m_{\delta_e}}$	-2.260	-0.78
$C_{l_{\delta_a}}$	0.172	0.0291

While Envoy 600's control derivatives are underpowered relative to the Cessna 310, it was deemed reasonable.

7.3 Stability Derivatives

Stability derivatives were analyzed using DATCOM. As there were no accurate estimate of the rotational mass properties of the Envoy 600 available, determination of stability was done purely through stability derivatives.

To ensure that that the values obtained from DATCOM was reasonable, the values were compared to that of Cessna 310 around climb, cruise, and approach conditions, obtained from Roskam [8].

7.3.1 Longitudinal Stability

For static longitudinal stability, coefficient of pitching moment caused by angle of attack, C_{m_α}, was analyzed. Table 7-5 shows the comparison of the stability derivatives.

Table 7-5 Comparison of Longitudinal Static Stability Coefficient

	Cessna 310	Envoy 600
Climb	-0.339	-0.736
Cruise	-0.137	-0.638
Approach	-0.619	-0.531

The negative C_{m_α} and relative similarity in magnitude indicates that the Envoy 600 is sufficiently longitudinally statically stable.

For longitudinal dynamic stability, coefficient of pitching moment caused by change in angle of attack $C_{m_{\dot{\alpha}}}$ was analyzed. Table 7-6 shows the comparison of the dynamic stability derivatives.

Table 7-6 Comparison of Longitudinal Dynamic Stability Coefficient

	Cessna 310	Envoy 600
Climb	-14.8	-3.26
Cruise	-12.7	-3.56
Approach	-11.4	-3.80

The negative $C_{m_{\dot{\alpha}}}$ indicates that Envoy 600 is longitudinally dynamically stable.

7.3.2 Lateral Stability

For static lateral stability, coefficient of lateral moment caused by roll rate, C_{l_p}, was analyzed. Table 7-7 shows the comparison of the stability derivatives.

Table 7-7 Comparison of Lateral Static Stability Coefficient

	Cessna 310	Envoy 600
Climb	-0.552	-0.177
Cruise	-0.551	-0.165
Approach	-0.566	-0.174

The negative C_{l_p} and the magnitude indicates the lateral static stability of the Envoy 600.

7.3.3 Directional Stability

For static directional stability, coefficient of yawing moment caused by sideslip angle, C_{n_β}, was calculated manually, as DATCOM outputted incorrect value due to Envoy 600's curved fuselage using the equation below.

$$C_{n_\beta} = \eta_v \frac{\ell_v S_v}{\mathrm{Sb}} a_v \left(1 + \frac{d\sigma}{d\beta}\right) - 2\frac{V}{Sb}$$

Table 7-8 shows the comparison of C_{n_β} between Cessna 310 and Envoy 600.

Table 7-8 Comparison of Directional Static Stability Coefficient

	Cessna 310	Envoy 600
Climb	0.155	0.312
Cruise	0.144	0.312
Approach	0.168	0.312

The positive C_{n_β} and the similarity in magnitude between Cessna 310 and Envoy 600 indicates the directional static stability of the Envoy 600.

8 STRUCTURAL & LOADS

8.1 Materials Selection

The design of the aircraft requires materials that are light weight, cost effective, and a relatively high strength. To meet these requirements, we chose graphite Epoxy, Aluminum 7075 and Aluminum 2024 as the potential material for the aircraft. Aluminum has been used in the aerospace industry for decades and composite materials such as graphite epoxy are seeing more uses in recent years. To further down select from these 3 materials a trade study was performed. The weight factors for the trade study was base off the design and request for proposal. Weight and cost are more important than the strength requirement for the design because the tensile and compressive strength of the potential materials all exceed the requirements by a large margin. So, strength has a weight factor of 0.1, and weight and material cost have a weight factor of 0.5 and 0.4 respectively. Weight has a slightly higher weight factor because operational cost of the aircraft will have a larger cost benefit as time goes on. Since graphite epoxy is light, the figures of merit for weight and cost are weight per volume and dollar per volume. To ensure the amount of material were similar for each figure of merit. Specific Ultimate Strength was used for the strength figure of merit. A scale from 1 to 5 these figures of merit was made with 1 being the worst and 5 being the best. This scale is shown in table 8-1 and the trade study is shown in table 8-2. The trade study showed that aluminum 2024 was the most suitable material because the graphite epoxy cost was too high, and the strength difference of the 2 aluminum did not matter.

Table 8-1 Scale for Material trade Study

	1	2	3	4	5
Specific Ultimate Tension Strength (Ksi/lb/in^3)	100-300	300-500	500-700	700-900	900+
Weight (weight/vol.) lb/in^3	0.500-.400	0.400-0.300	0.300-.200	0.200-.100	<.100
Raw material cost (dollar/vol.) \$/in^3	\$4.00+	\$4.00-\$3.00	\$3.00-\$2.00	\$2.00-\$1.00	<\$1.00

Table 8-2 Material Trade Study

Materials/Figures of merit	Aluminum Alloy (7075)	Graphite Epoxy	Aluminum (2024)	Weight Factor (0-1)
Specific Ultimate Tension Strength (Ksi/lb/in^3)	4 (745)	5 (1105)	3 (630)	0.1
Weight (weight/vol.)	4 (.102lb/in^3)	5 (0.057lb/in^3)	4 (.100lb/in^3)	0.5
Raw material cost (dollar/vol.)	4 \$(1.26)/in^3	1 \$(40.97)/in^3	5 \$(0.76)/in^3	0.4
Weighted Total	4	3.4	4.3	1

8.2 Aircraft Loads

8.2.1 V-n Diagram

The Velocity-Load factor diagram is made with a combination of equations from Fundamentals of Aircraft Design volume 1 and limits set by the Federal Aviation Regulations part 23. This is done to find the maximum structural limit of the aircraft. The equations used were found from Fundamentals of Aircraft Design Volume 1 [1] and FAR 23.

These equations are used to make a MATLAB with following inputs. The altitude is set to 8000 feet, MTOW as 3434 pounds, $C_{L_{max}}$ is 1.637 and the true air speed is set to 206 knots. The aircraft's cruise speed is assumed to be the true air speed of the aircraft for our analysis. After running the MATLAB program, the V-n diagram is plotted below in figure 8.2.1-1.

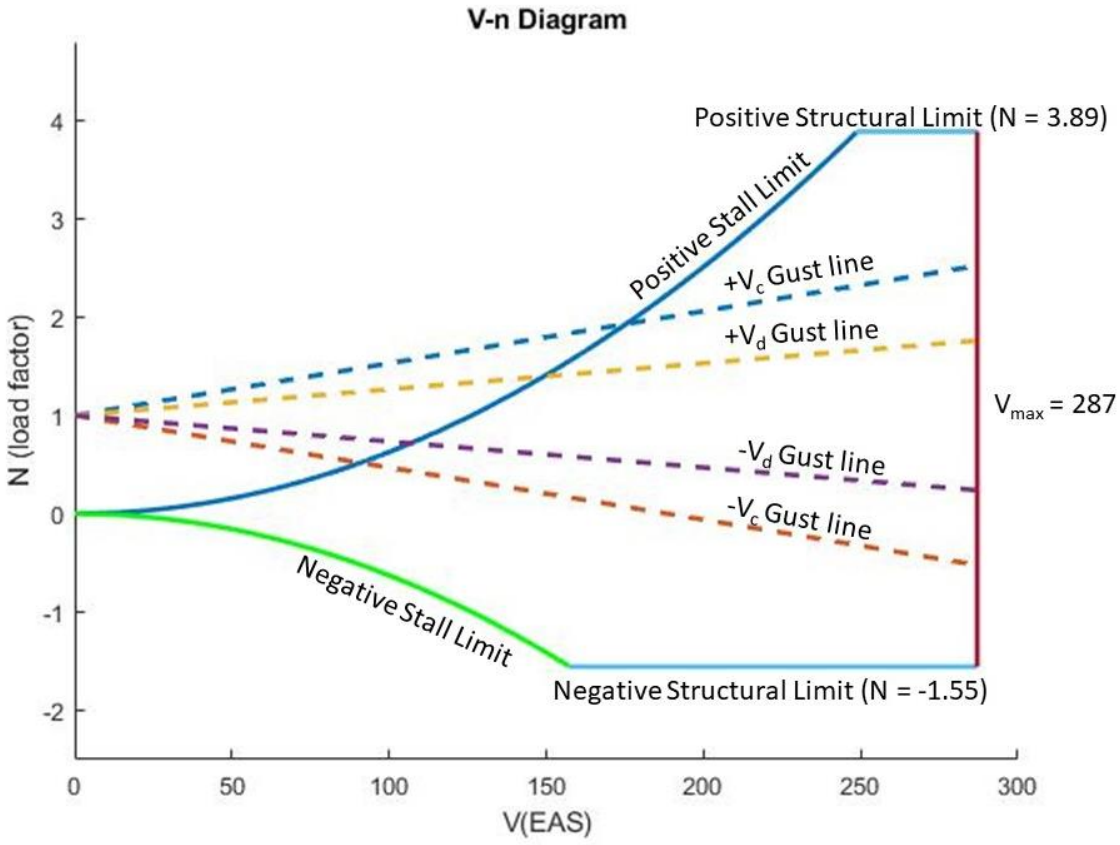

Figure 8.2-1 V-n Diagram

8.3 Internal Structural Element Layout

8.3.1 Fuselage Structure

It was decided to use 4 stringers at the top and bottom corners of the fuselage, so the structural strength is constant for the entire fuselage. The shape of the stringer was selected to be an I-beam because of its' ability to handle bending and shear loading. To ensure that the fuselage will not fail due to bending or shear during flight, several assumptions were made for this analysis. First it was assumed that all the loading would be handled by the stringer and the skin of the aircraft carried no load. This was done because the aircraft is designed to an altitude of 8000 feet. At this altitude, the passenger cabin does not need to be pressurized and it allowed us to be more conservative in our calculations. In compliance with the Federal Aviation Regulations requirements for manned aircraft, a factory of safety of 1.5 was applied to the calculations. To account for the worst-case scenario the positive structural limit was also applied to the calculations. Using the book Analysis and Design of Flight Vehicle Structures, Bruhn [13] provides a simple equation to calculate the total cross-sectional area of the stringer and effective area of the skin for a circular or elliptical fuselage.

$$M_y = A_c(0.67\sigma_b)(0.75H) \qquad \text{(Bruhn Ch.20)}$$

Moving the variables around the equation transform into the following below.

$$A_C = \frac{M_y}{(0.67\sigma_b)(0.75H)}$$

Where M_y has a value of 2224150.29 lb-in, H is 64 inches, and the ultimate compressive allowable σ_b has a value of 41 Ksi. The total cross-sectional area needed to withstand the load is about 1.687 square inches. Since the design fuselage is square shape instead of circular, the cross-sectional area of each stringer was increase by about 0.1 square inches. Therefore, each stringer will have a cross

sectional area of about 0.54 square inches. The dimension of the stringer is shown in the figure below.

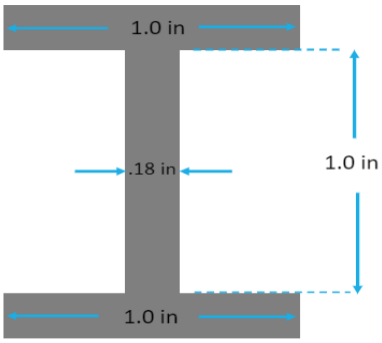

Figure 8.3-1 Stringer Dimensions

A cross section of the design fuselage was modeled in FEMAP using rod, bar and shear elements. In the FEMAP model, the rod elements were used to model the stringers and bar elements were used for the frames in the fuselage to keep the stringers from rotating. The material properties are shown in Table 8-3. While the properties for the stringer and shear panel are in Table 8-4, the properties for the frames and wagon wheel are in Tables 8-5 and 8-6 respectively. These frames were placed every 1.5 feet going into the fuselage from the nose. The shear elements are used to model the skin of the aircraft. Lastly, a wagon wheel made of Cbar elements with zero mass and an extremely large stiffness was used to constrain one end of the fuselage and apply the moment load on the other end. The fuselage cross section is modeled at the center of gravity of the aircraft because Bruhn [13] states that the loading on fuselage are made of point loads, and the largest point load happens to be at the center of gravity. The analysis of the FEMAP model shows that the moment load with the positive structural limit and factory of safety applied only moved the fuselage by 0.198 inches. This result is shown in Figure 8.3.1-2. Therefore, it can be concluded that the stringers will hold the load. The overall wing structure can be seen in Figure 8.3.1-3.

Table 8-3 Material Properties

Material Properties	
Young Modulus, E	10500000
Shear Modulus, G	4000000
Poisson's Ratio	0.33

Table 8-4 Stringer and Shear Panel Properties

Stringer properties	
Area, A	0.54
Torsional Constant, J	0.005832
Shear Panel Properties (skin)	
Thickness, t	0
Nonstructural Mass/area	0

Table 8-5 Frame Properties

Frames Properties	
Area, A	5.0
Moment of Inertia, I1	0.5
I2	0.5
Torsional Constant, J	0.08525

Table 8-6 Wagon wheel Properties

Wagon wheel Properties	
Area, A	0.002
Moment of Inertia, I1	200000
I2	20
I12	0
Torsional Constant, J	0.2

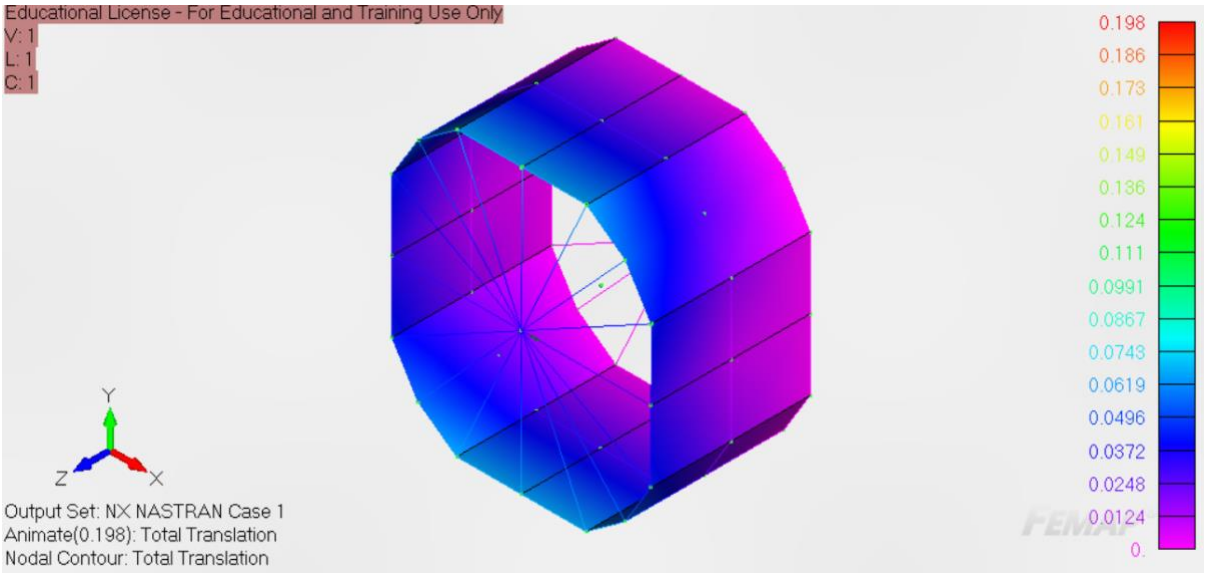

Figure 8.3.1-2 FEMAP model results

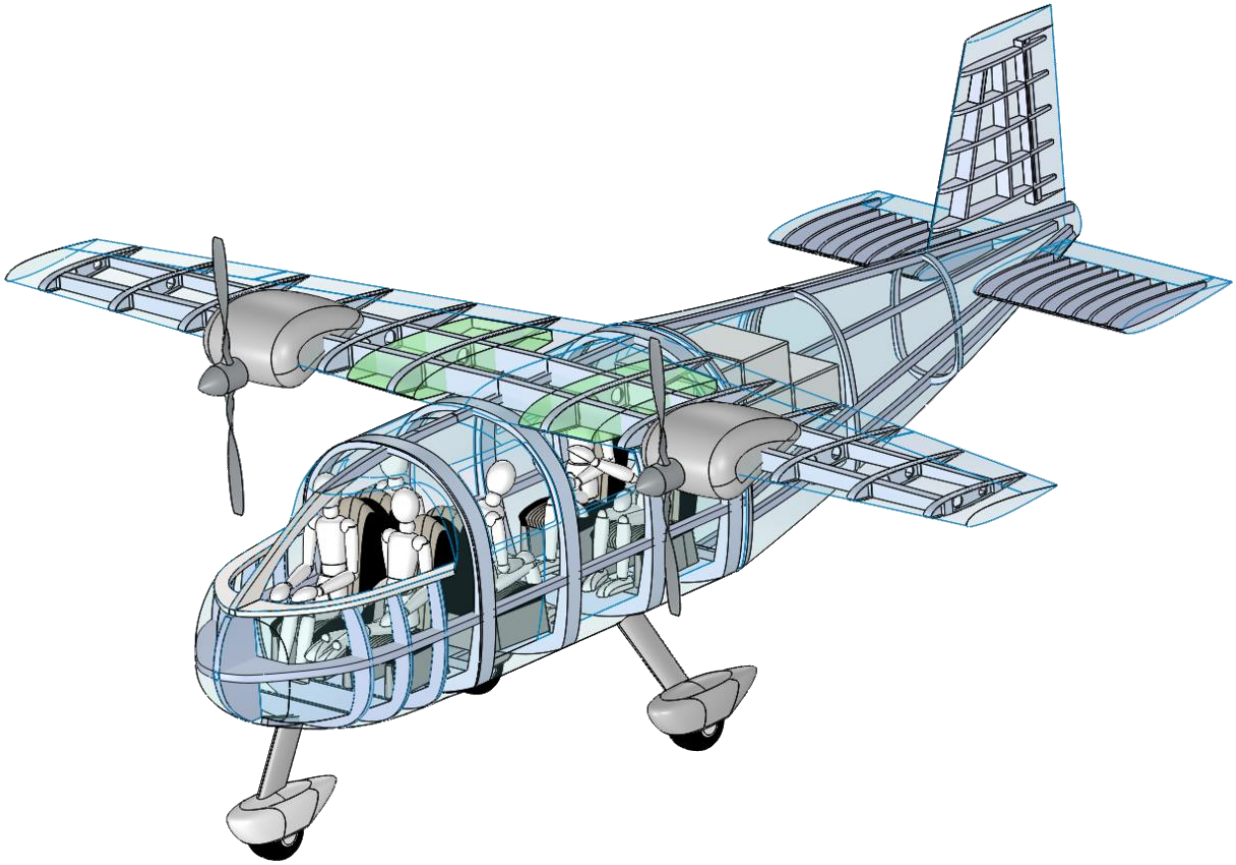

Figure 8.3.1-3 Envoy 600 Skeleton

8.4 Landing Gear

One key parameter for our design was to decide what kind of landing gear type was the best option to integrate to the aircraft. Because the velocity at which the aircraft is going is not substantial and the space in the aircraft is limited for a retractable landing gear, we decided to integrate a fixed, tricycle landing gear. In addition, we decided to put fairings on the landing gear to reduce the drag that the fixed landing gear produces. The main landing gear holds 85% of the maximum takeoff weight (MTOW), behind the center of gravity, and in front of the neutral point, so the aircraft does not tip back. In regard to the nose landing gear, according to Ref. [3], the nose landing gear must hold 15-20% of the MTOW; therefore, the nose landing gear for our design holds 15% of the MTOW. Figure 8.4-1 illustrates the position of the landing gear on the aircraft and the tip back and main gear relative to CG angle.

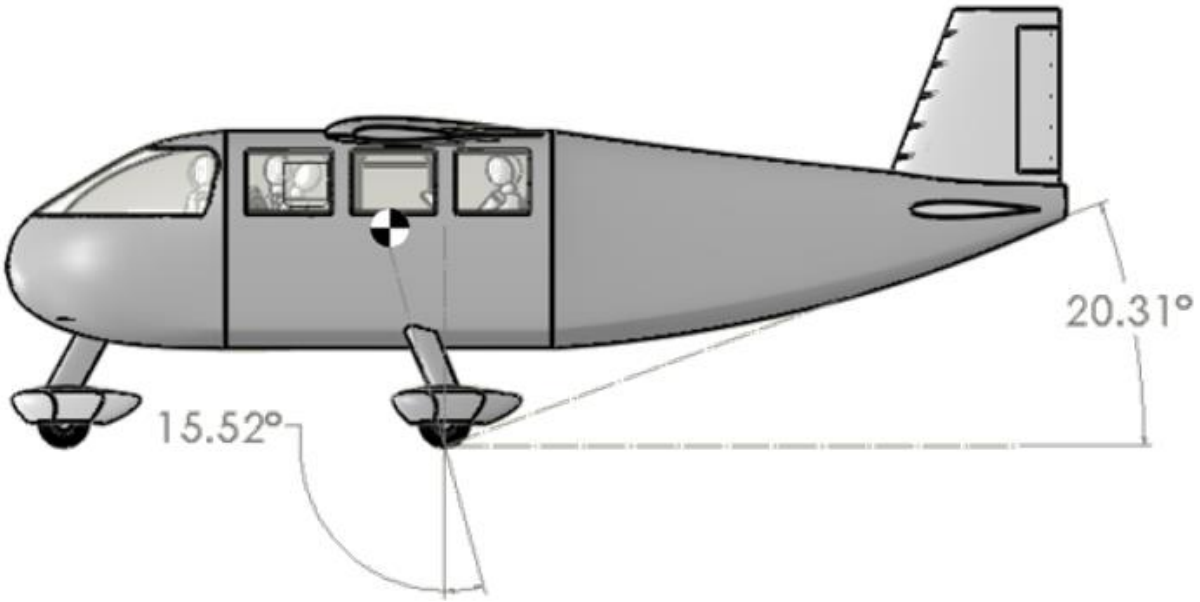

Figure 8.4-1 Landing Gear tip-back and Main gear relative to CG angle

8.4.1 Tire Sizing

For the aircraft tire selection, Ref. [9] was used to determine the tire sizing by determining the loads on the nose and main gear. Per Raymer, a margin of 25% was accounted for future growth

of the aircraft design. Once the aircraft gear loads were determined, tires were selected from the Goodyear aircraft tire series [2]. The resulting tires were chosen for both the main gear and the nose gear as seen in Table 8-7.

Table 8-7 Tires for Landing Gear

Tire Sizing	**MLG**	**NLG**
Type	III	III
Size	7.00-8	5.00-5
Rated Load (lbs)	6750	1285
Inflation for paved runway (psi)	128	50
Diameter (in)	21.36	14.2
Width (in)	7.59	4.95

9 WEIGHTS & BALANCE

9.1 Major Component Weights & Locations

The major component weights of the aircraft were calculated using the weight estimation formulas from the revised Chapter 20 of reference [5] for a light utility aircraft. Table 9-1 and 9-2 show the weight estimations considered for our particular design, as well as, their location in the longitudinal and vertical axis. The datum used to locate the major components on our design was from the nose of the fuselage and the bottom of the fuselage for the longitudinal and vertical axis, respectively. Furthermore, the Class I Weight and Balance Method from Ref. [8] was used to find the locations of the major components.

Table 9-1 Component Weights and Location for X_{cg}

No. Type of Component	W_i (lb.)	x_i (in.)
1. Fuselage	369	121.7
2. Wing	260	112.5
3. Horizontal tail	36.1	279.6
4. Vertical tail	16.1	283.7
5. Engine	784	107.9
6.1 Main LG	154	129.7

6.2 Nose LG	27.1	16.2
7.1 Surface controls	89.9	140
7.2 Electrical System	7.47	44.3
7.3 Instrumentation, avionics, and electronics	55.2	44.3
7.4 Fuel System	39.9	112.5
7.5 Furnishings (Row1)	49.7	50
7.6 Furnishings (Row 2)	49.7	80.8
7.7 Furnishings (Row 3)	49.7	140.8
8. Trapped fuel and oil	4.66	114.3
9. Crew	180	50
10. Fuel	237	114.3
11.1 Passengers (Row 1)	180	50
11.2 Passengers (Row 2)	360	80.8
11.3 Passengers (Row 3)	360	140.8
12. Baggage	125	200

The x_{cg} was calculated by equation 9.1.1 below:

$$x_{cg} = \frac{\sum W_i x_i}{\sum W_i} \qquad \text{Eqn. 9.1.1}$$

The x_{cg} location for our design is located at 9.12 ft. from the nose of the fuselage.

Table 9-2 Component Weights and Location for Z_{cg}

No. Type of Component	W_i (lb.)	z_i (in.)
1. Fuselage	369	31.9
2. Wing	260	55.9
3. Horizontal tail	36.1	63.9
4. Vertical tail	16.1	95.9
5. Engine	784	47.5
6.1 Main LG	154	-29.2
6.2 Nose LG	27.1	-29.2
7.1 Surface controls	89.9	61.2
7.2 Electrical System	7.47	19.2
7.3 Instrumentation, avionics, and electronics	55.2	19.2
7.4 Fuel System	39.9	54
7.5 Furnishings (Row 1)	49.7	26.4
7.6 Furnishings (Row 2)	49.7	26.4
7.7 Furnishings (Row 3)	49.7	26.4
8. Trapped fuel and oil	4.66	54

9. Crew	180	26.4
10. Fuel	237	54
11.1 Passengers (Row 1)	180	26.4
11.2 Passengers (Row 2)	360	26.4
11.3 Passengers (Row 3)	360	26.4
12. Baggage	125	25.2

The z_{cg} was calculated by following equation 9.1.2:

$$z_{cg} = \frac{\sum W_i z_i}{\sum W_i} \qquad \text{Eqn. 9.1.2}$$

The z_{cg} location for our design is located at 2.84 ft. from the bottom of the fuselage.

9.2 Center of Gravity Envelope

In flight, the center of gravity (CG) shifts during the course of the mission. As fuel is burned over the course of the mission, the CG shifts away from the takeoff CG location. Figure 9.2-1 illustrates the change in CG for four different cases of travel. The CG locations are represented by percent of the mean aerodynamic chord (MAC). As seen in Figure 9.2-1, the most forward CG that Envoy experiences will be during full standard mission. The most aft CG location will be experienced at operating empty weight landing.

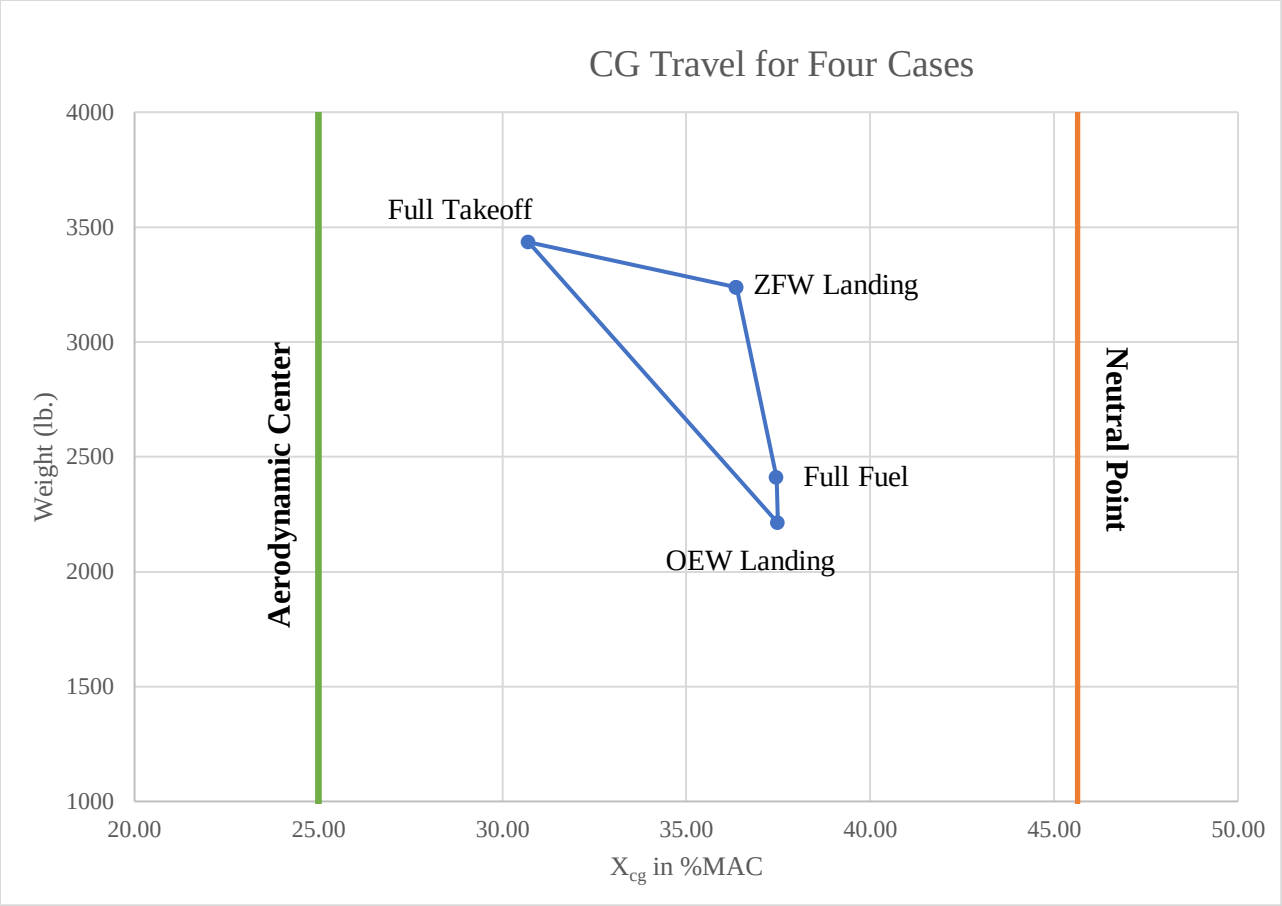

Figure 9.2-1 CG Travel for Four Cases

As seen in the figure 9.2-1, the CG lies within the aerodynamic center (AC) and the neutral point (NP) of the aircraft. The position of the CG relative to the NP and the AC indicates the stability of the aircraft. The static margins are used to assess the stability of the aircraft. In addition, to meet stability requirements, the static margin needs to lie within 5-15%. The four CG cases can be seen in Table 9-3 with the resulting static margins. As seen, the static margins range from 8-15% which fall within the range for stability.

Table 9-3 Center of Gravity Travel Static Margins

Mission Segment	Weight (lb.)	Static Margin (%)
Operating Empty Weight	2,212	8.2
Zero Fuel Weight	3,235	9.3
Full Fuel, No Payload	2,409	8.2
Full Takeoff	3,434	14.9

10 COST ANALYSIS

10.1 Initial Cost Estimate & Breakdown

To get an accurate cost estimate for our design, we needed a method that applied more appropriately to civilian aircraft. Methods, such as the DAPCA IV model developed by the RAND corporation, found in Ref. [7], used historical data on military which when applied to real civilian aircraft were found to overestimate the cost by over three times. The Eastlake model was developed specifically for civilian aircraft cost estimation. The Eastlake model is a modification of the DAPCA IV. It uses the DAPCA IV equations as a base line. Then, uses a weight factor based on the authors experience in industry. A final round of weight factors is used to calibrate the estimate as close to the actual cost as possible. The Eastlake Model is what we used to calculate our cost estimates.

10.1.1 Research, Development, Testing & Evaluation Costs

The wrap rates found used in Raymer [7] are used to calculate the direct cost of labor including salaries, benefits, overhead, and administrative costs. The wrap rates given are in 1984 dollars and are then adjusted to 2019 dollars.

Table 10-1 Wrap Rates for Labor Per Hour

LABOR AREA	**WRAP RATES (1984)**	**WRAP RATES (2019)**
ENGINEERING	$59.10	$143.02
TOOLING	$60.70	$146.89
QUALITY CONTROL	$55.40	$134.07
MANUFACTURING	$50.10	$121.24

The number of hours in each area were then found using the equations provided in the DAPCA model. The hours are based on several different parameters of our design such as aircraft weight, speed, and potential production quantity. These hours are multiplied with the adjusted wrap rates from Table 10-2 to gather the estimated labor area cost.

Table 10-2 Cost for Labor (in millions)

LABOR	500 units	1000 units	2000 units
Engineering	$123.9	$138.7	$155.3
Tooling	$12.2	$14.7	$17.6
Manufacturing	$49.4	$77.0	$120.1
Quality Control	$7.26	$11.3	$17.7
Total	$192.7	$241.7	$310.6

The second part of the total cost comes from the Development Support, Flight Testing, Manufacturing Materials, and Engine costs. These values were found from the DAPCA IV model. These equations relied on some of our design parameters. The Engine cost was based on acquisition cost of an off the shelf engine rather than the development. In our case, we used the Lycoming IO-360-A1A which costs approximately $58,000. Since our aircraft is dual engine, we add a fix cost of $116,000 to each aircraft. We also add the cost to acquire avionics for our aircraft which is approximately $50,000 per aircraft. Table 10-3 shows the costs of each of these areas.

Table 10-3 Development Support, Flight Test, Materials, & Engine Costs (in millions)

Area	500 units	1000 units	2000 units
Development Support	$8.65	$8.65	$8.65
Flight Test	$3.51	$3.51	$3.51
Manufacturing Materials	$2.20	$3.84	$6.67
Quality Control	$7.26	$11.33	$17.66
Engine Cost	$58.00	$116.00	$232.00
Total	$79.62	$143.33	$268.49

With every major cost area estimated, we summed all the values and calculated the total program cost based on the projected number of units sold. This can be seen in the table below.

Table 10-4 Overall Program Cost (in millions)

Overall Program Cost	500 units	1000 units	2000 units
Total	$290.1	$423.7	$661.4

10.1.2 Flyaway Cost

The aircraft flyway cost is the estimated cost for producing or manufacturing an aircraft. This includes manufacturing labor, manufacturing materials, quality control, the avionics, and engine costs. This often excludes the Research, Development, Testing & Evaluation costs of the program. The Eastlake model was used to estimate the relevant costs at 500, 1000, and 2000 production units.

Table 10-5 Production Breakdown (in millions)

AREA	500 Units	1000 Units	2000 Units
Manufacturing Labor	$49.3	$77.0	$120.0
Manufacturing Materials	$2.20	$3.84	$6.67
Quality Control	$7.26	$11.33	$17.66
Avionics	$25.0	$50.0	$100.0
Engines	$58.0	$116.0	$232.0
Production Total	$141.76	$258.33	$476.33

Table 10-6 Flyaway Cost (in thousands)

	500 Units	1000 Units	2000 Units
Flyaway Cost	$283.7	$258.2	$238.2

10.1.3 Sell Price for 20% Profit

To establish a sell price, added the flyaway costs found in the previous section and the development cost of the aircraft. The development costs were divided among the number of units we project to be produced. With the development costs being relatively fixed, the more number of units produced the cheaper the aircraft will be. To turn a profit, a 20% profit margin was added to the cost to get the final sell price of the aircraft.

Table 10-7 Sell Price for 20% Profit (in thousands)

	500 Units	1000 Units	2000 Units
Flyaway Cost	$283.7	$258.2	$238.2
RDT&E	$296.4	$165.5	$92.5
Purchase Cost	$696.2	$508.4	$396.9

10.2 Operations & Maintenance Cost Considerations

10.2.1 Fuel Costs

The fuel cost was found using the average cost of Avgas across the country and our burn rate during the mission. The cost of a single gallon of Avgas was $5.04. With a burn rate of approximately 32.6 gal/hr, we estimate that the cost be $164.25 per hour in fuel for both the reference mission and sizing mission.

10.2.2 Crew Salaries

The crew salary was estimated using the Crew Salary equation found in Raymer. This equation takes into account the gross weight and cruise velocity of our aircraft. Due to the fact we only need one pilot in our aircraft we used the Two-Crew equation and divided it in half to get the cost. Our cost per flight hour is approximately $73 per flight hour.

10.2.3 Maintenance Expenses

The estimated maintenance expenses for the aircraft were estimated using equations outlined by Tony Hays [Ref. 15]. This method breaks down the maintenance into Airframe Maintenance and Engine Overhaul. Each area has an associated labor and materials cost that contributes to the overall cost on maintenance. Table 10-8 shows the estimated cost breakdown and the total cost per flight hour for our aircraft.

Table 10-8 Aircraft Maintenance Breakdown & Total Cost per flight hour

Airframe Maintenance Labor	$95.70
Airframe Maintenance Materials	$67.17
Engine Overhaul Labor	$38.29
Engine Overhaul Materials	$73.54
Total Per Hour	$274.70

10.2.4 Yearly Maintenance & Operation Costs

The yearly direct operating cost was found using the associated costs of fuel, crew, & maintenance cost per flight hour and multiplying it with the project flight hours in a year. The yearly cost was estimated for 750 and 1000 flight hours which are the projected hours for different combinations of sizing and reference mission flights in a year. The values can be found below in Table 10-9 and Table 10-10. The yearly operating costs of the Piper M600 & Cessna 208 from [6] are also displayed for comparison.

Table 10-9 Yearly Direct Operating Costs for 750 Flight Hours (in thousands)

Aircraft	Envoy 600	Piper M600	Cessna 208
Fuel	$123.2	$161.3	$158.9
Maintenance	$122.2	$101.3	$88.5
Engine Overhaul	$83.9	$105.0	$90.8
Crew	$54.8	$93.8	$93.8
Total Per Hour	$384.0	$461.3	$431.3

Table 10-10 Yearly Direct Operating Costs for 1000 Flight Hours (in thousands)

Aircraft	Envoy 600	Piper M600	Cessna 208
Fuel	$164.3	$215.0	$211.0
Maintenance	$162.9	$135.0	$118.0
Engine Overhaul	$111.8	$140.0	$121.0
Crew	$73.0	$125.0	$125.0
Total Per Hour	$512.0	$615.0	$575.0

Based on Prijet's [6] average total hourly cost of thin haul aircraft shown in Figure 10.2-1, as the annual flight hours increase, the price per hour decreases until it plateaus after a certain amount of flight hours. This decrease is mostly due to the distribution of maintenance and operating cost among a higher number of flights. As previously mentioned, the Envoy 600 is estimated to operate anywhere between 750 and 1000 hours yearly, which is the best and most profitable range of

operation. This results in a cost-per-seat mile of about 0.56¢ which is below the thin haul aircraft average.

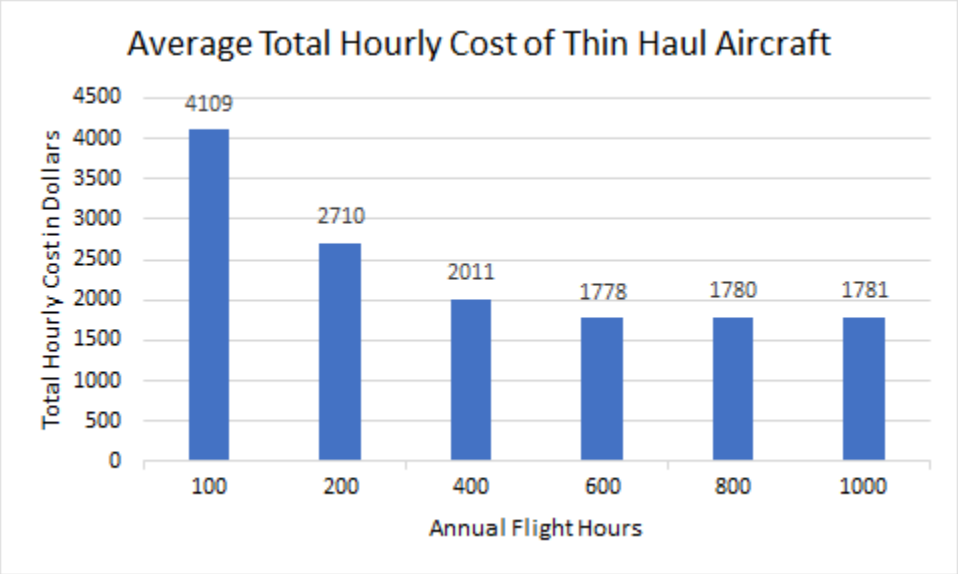

Figure 10.2-1 Average Total Hourly Cost of Thin Haul Aircraft

11 TECHNOLOGY READINESS LEVEL

The request for proposal requires all technology employed on the aircraft to meet technology readiness level (TRL) 7. In Table 11-1 below, TRL compliance matrix is shown, demonstrating that all major technology groups on the aircraft meets this requirement.

Table 11-1 Technology Readiness Level Compliance Matrix

Technology	TRL
Twin Piston Engine Propulsion System	9
Aluminum Structure	9
Integrated Fuel Tank	9
Control System	9

12 CONCLUSION

With the rapid advancement in aviation technology, the emerging demand for the aircraft taxi market has the potential for exponential growth. Envoy 600's low acquisition cost and direct operating cost makes it an attractive choice for many operators, both small and large who wishes to exploit the new market. Its proven technologies allow for easy maintenance, repair, and replacement of components, and ensure that the aircraft will be operational for a long time.

Envoy 600 currently meets all the requirements set by the request for proposal, as well as current FAA regulations regarding small passenger aircraft. With increased passenger comfort provided by low noise, large cabin space, and stable flight dynamics, Envoy 600 is a competitive choice in the thin haul aircraft market.

APPENDIX A COMPLIANCE MATRIX

Description	Requirement	Section
Passenger Capacity	2-6 passengers	Section 2.1, 3.5.2
Cargo Capacity	Luggage space for 2-6 people	Section 3.5.4
Reference Mission Minimum Cruise Speed	180 kts	Section 4.1, 4.6
Reference Mission Range (1/2 payload)	min. 135 nmi	Section 4.1
Reference Mission Ground Speed for Cruise	Max. 45 min	Section 4.1
Sizing Mission Range (full payload)	min. 250 nmi	Section 4.1
Takeoff/Land over obstacle	50 ft	Section 4.3
Takeoff & Landing Length	Max 2500 ft for both takeoff & landing	Section 4.3
Technology Readiness	Technologies must be available by 2025	Section 11.1
Regulation	Meets certification rules in FAA 14 CFR Part 23	Section 4.8,
Crew Capacity	Aircraft must contain 1 pilot	Section 2.1, 3.5.2
Engine Noise limits	Aircraft must meet single engine noise limits even if multi-engine (Part 36 Sec. G36.301(c)	Section 4.8
Direct Operating Costs lower than current industry	$431/hr (Based on Cessna 208)	Section 10.2
Battery specific energy	No greater than 285 W-hr/kg - Px85 s	N/A
Battery overhaul cost	Minimum $250 per kW-hr every 1000 cycles	N/A
Cost of electricity	Minimum $0.10 /kW-hr	N/A

APPENDIX B REFERENCES

[1] Abbott I. H., von Doenhoff A. E., and Strives Jr L. S., *SUMMARY OF AIRFOIL DATA*. NACA report no. 824, 1945.

[2] Goodyear. *Global Aviation Tires*. https://www.goodyearaviation.com/resources/pdf/databook_7_2016.pdf.

[3] NACA 0012 image - http://www.airfoildb.com/airfoils/435

[4] NACA 23012 image - http://airfoiltools.com/airfoil/details?airfoil=naca23012-il

[5] Nicolai L. M. and Carichner G. E., *Fundamentals of Aircraft and Airship Design Volume I*. AIAA 2010.

[6] Prijet Aircraft Performance and Specifications -https://prijet.com/

[7] Raymer, D. P., *Aircraft design: a conceptual approach*. AIAA 6th ed., 2018.

[8] Roskam, Jan. *Airplane Flight Dynamics and Automatic Flight Controls, Part 1*. Lawrence, Kansas, Design, Analysis and Research Corporation, 1998

[9] Roskam, Jan. *Part II: Preliminary Configuration Design and Integration of the Propulsion System*. 4th ed., vol. 2, Lawrence, Kansas, Design, Analysis and Research Corporation, 1985, 8 vols

[9] Roskam, Jan. *Part V: Component Weight Estimation.* 3rd ed., vol. 5, Lawrence, Kansas, Design, Analysis and Research Corporation, 1985, 8 vols

[10] Torenbeek, E., *Synthesis of Subsonic Airplane Design.* Delft University Press. Dordrecht, The Netherlands, 1982.

[11] EMRAX. *EMRAX 268 / 268 VHML Technical Data Table (dynamometer test data)*, https://emrax.com/wp-content/uploads/2017/01/emrax_268_technical_data_4.5.pdf

[12] Kokam, *Kokam Cell Brochure V.2*. http://kokam.com/data/Kokam_Cell_Brochure_V_2.compressed.pdf

[13] Bruhn, E. F. *Analysis and Design of Flight Vehicle Structures*. Tri-State Offset, 1973.

[14] FAR 36 Appendix G 36.301c

[15] Tony Hayes, "Aircraft and Airline Economics," www.adac.aero/Documents/Raymer_Annotations/18.7_Aircraft_and_Airline_Economics.pdf